

Wave Attenuation Performance of Improved Wave Suppress System (IWSS)

by

Nuzul Izani binti Mohammed

Dissertation submitted in partial fulfilment of
the requirements for the
Bachelor of Engineering (Hons)
(Civil Engineering)

DECEMBER 2005

Universiti Teknologi PETRONAS
Bandar Seri Iskandar
31750 Tronoh
Perak Darul Ridzuan

CERTIFICATION OF APPROVAL

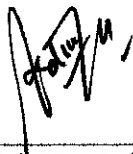
Wave Attenuation Performance of Improved Wave Suppress System (IWSS)

by

Nuzul Izani binti Mohammed

A project dissertation submitted to the
Civil Engineering Programme
Universiti Teknologi PETRONAS
in partial fulfilment of the requirement for the
BACHELOR OF ENGINEERING (Hons)
(CIVIL ENGINEERING)

Approved by,



(Mr. Teh Hee Min)

UNIVERSITI TEKNOLOGI PETRONAS

TRONOH, PERAK

December 2005

CERTIFICATION OF ORIGINALITY

This is to certify that I am responsible for the work submitted in this project, that the original work is my own except as specified in the references and acknowledgements, and that the original work contained herein have not been undertaken or done by unspecified sources or persons.



NUZUL IZANI BINTI MOHAMMED

ABSTRACT

Wave attenuation performance of Improved Wave Suppress System (IWSS); a floating breakwater system used to dissipate wave energy, has been studied in this project. For the first semester, IWSS has been designed and developed to enhance wave attenuation performance of the existing Wave Suppress System (WSS). Experimental studies have been carried out for the calibration of wave period, and determination of attenuation performance of WSS and IWSS in terms of reflection coefficient, C_r , transmission coefficient, C_t , and loss coefficient, C_l in various water depths and stroke adjustments. From the experimental result and analysis, it is found that WSS is not a good reflector but indeed a good dissipator, as it is capable in attenuating up to 96% of wave energy. The results also show that IWSS models produced lower C_t values compared to WSS. The addition of keel plate underneath IWSS has increased the draft of the structure, thus enhanced the attenuation performance of the breakwater. It can be concluded that IWSS with keel plate is a good reflector as it has improved the wave reflection ability. WSS and IWSS models performed very well in 20 cm water depth and short wave period. Comparison of WSS and IWSS models with previous studies indicates that draft and width has significant effect on the performance of floating breakwater.

ACKNOWLEDGEMENT

The author would like to express her gratitude to the supervisor, Mr. Teh Hee Min; lecturer of Civil Engineering Department, Universiti Teknologi PETRONAS for the guidance throughout this project. Thank you for the supports and motivation.

To my friends; Wong Siew Lee and Mohd Irwan Mohd Saari, thank you for all the helps during experimental works. Your contributions are highly appreciated.

To my family, thank you for your prayers and moral support. The author is more excited to complete this project successfully.

Last but not least, million of thanks to lecturers, technicians and classmates who contribute in this project directly or indirectly.

Thank you.

NUZUL IZANI MOHAMMED (2549)

Civil Engineering

TABLE OF CONTENT

ABSTRACT	i
ACKNOWLEDGEMENTS	ii
SYMBOLS	v
LIST OF FIGURES	v
LIST OF PLATES	vii
LIST OF TABLES	vii
CHAPTER 1: INTRODUCTION	1
1.1 Background of Study	1
1.2 Problem Statement	2
1.3 Significance of the Study	3
1.4 Objective of the Study	4
1.5 Scope of Study	5
CHAPTER 2: LITERATURE REVIEW	6
2.1 Wave Breaking, Wave Run-up, and Wave Overtopping	6
2.2 Wave Reflection	7
2.3 Wave Transmission	8
2.4 Energy Loss	8
2.5 Performance of Existing Floating Breakwater	9
2.5.1 Various Floating Breakwaters Configurations	9
2.5.2 Cage Floating Breakwater (CFB)	13
2.5.3 Freely Floating Porous Box	15
2.5.4 Wave Suppress System (WSS)	17
2.5.5 Comparison of Existing Breakwaters Performance	19
2.6 Floating Breakwater Design Criteria	20

CHAPTER 3: IMPROVED WAVE SUPPRESS SYSTEM (IWSS)	21
3.1 Introduction	21
3.2 Development of IWSS	21
3.3 Description of IWSS	21
3.4 Conceptual Wave Dissipation Mechanism of IWSS	24
CHAPTER 4: EXPERIMENTAL SET UP AND PROCEDURE	26
4.1 Introduction	26
4.2 Laboratory Equipment and Instrumentation	26
4.3 Experimental Procedures	28
4.3.1 Preliminary Test	29
4.3.2 Experimental Studies on IWSS	30
CHAPTER 5: EXPERIMENTAL RESULTS AND DISCUSSION	31
5.1 Introduction	31
5.2 Determination of Wave Period, T	31
5.3 Determination of Incident Wave height, H_i	33
5.4 Wave Suppress System (WSS)	36
5.5 Improved Wave Suppress System (IWSS)	39
5.6 Improved Wave Suppress System with keel plate	41
5.7 Comparison of WSS and IWSS performances	44
5.8 Determination of Wavelength, L .	50
5.9 Comparison of Performance of IWSS with Previous Studies	53
CHAPTER 6: CONCLUSION AND RECOMMENDATION	55
6.1 Conclusion	55
6.2 Recommendation	57
REFERENCES	58
APPENDICES	60

SYMBOLS

H_i	incident wave height	E_i	wave energy
H_r	reflected wave height	E_r	reflected wave energy
H_t	transmitted wave height	E_t	transmitted wave energy
C_r	reflection coefficient	E_l	energy loss
C_t	transmission coefficient	H_i/gT^2	wave steepness
C_l	loss coefficient	f	stroke frequency
T	wave period	S	stroke duration
W	width of breakwater	D/d	draft-to-water depth ratio
h	height of breakwater	L	wavelength
l	length of breakwater	d/L	relative depth
D	draft	W/L	width-to-wavelength ratio
d	water depth		

LIST OF FIGURES

Figure 2.1 :Types of wave height; incident wave height (H_i), reflected wave height (H_r), and transmitted wave height (H_t).

Figure 2.2 : Model 1 to 6 and its transmission coefficients. (Source: COPEDEC III Third International Conference on Coastal and Port Engineering in Developing Countries Mombassa, Kenya).

Figure 2.3 : Model 7 to 11 and its transmission coefficients. (Source: COPEDEC III Third International Conference on Coastal and Port Engineering in Developing Countries Mombassa, Kenya).

Figure 2.4 : Model 12 to 16 and its transmission coefficients. (Source: COPEDEC III– Third International Conference on Coastal and Port Engineering in Developing Countries Mombassa, Kenya).

Figure 2.5 : Cage floating breakwater. (Murali and Mani, 1997).

Figure 2.6 : Variation of transmission and reflection coefficients. (Murali and Mani, 1997).

Figure 2.7 : Performance of various studies of floating breakwater. (Murali and Mani, 1997).

Figure 2.8 : Schematic diagram of floating porous box. (Drimer and Stiassnie, 1992).

Figure 2.9 : Comparison of performance between a porous fixed box (...), a porous free box (---) and an impermeable free box (—). (Drimer and Stiassnie, 1992).

Figure 2.10: Wave Suppress System.

Figure 2.11: Transmission coefficient of WSS.

Figure 2.12: Comparison of Floating Breakwater Performance.

Figure 3.1 : Cross section of IWSS. The length is 30cm.

Figure 3.2 : a) Isometric view and b) side view of IWSS.

Figure 3.3 : Wave dissipation mechanism of IWSS.

Figure 5.1 : Observed wave period for 80 mm, 140 mm, and 200 mm stroke adjustments.

Figure 5.2 : Stroke duration vs average observed wave period.

Figure 5.3 : Incident wave height for 3 water depths; a) 20cm, b) 25cm, and c) 30cm.

Figure 5.4 : Reflection coefficient, Transmission coefficient, and Loss coefficient for WSS system.

Figure 5.5: Reflection coefficient, Transmission coefficient, and Loss coefficient for IWSS system.

Figure 5.6: Reflection coefficient, Transmission coefficient, and Loss coefficient for IWSS with keel plate system.

Figure 5.7: Reflection coefficients for a) 20 cm, b) 25 cm, and c) 30 cm water depth.

Figure 5.8: Transmission coefficients for a) 20 cm, b) 25 cm, and c) 30 cm water depth.

Figure 5.9: Loss coefficients for a) 20 cm, b) 25 cm, and c) 30 cm water depth.

Figure 5.10: Classification of water condition.

Figure 5.11: Comparison of Transmission Coefficient results with previous studies.

LIST OF PLATES

Plate 3.1: Model of IWSS.

Plate 3.2: Keel plate.

Plate 4.1: Wave flume.

Plate 4.2: wave paddle.

Plate 4.3: Wave generator and switch box.

Plate 4.4: Hook and point gauge.

Plate 4.5: Side view of wave absorber.

Plate 4.6: Placement of wave absorber in the wave flume.

Plate 5.1: Wave dissipation mechanism of IWSS.

Plate 5.2: Higher wave reflection for IWSS with keel plate.

LIST OF TABLES

Table 3.1: Nominal properties of Autoclaved Lightweight Concrete.

Table 5.1: Observed wave period for 80 mm, 140 mm, and 200 mm stroke adjustment.

Table 5.2: Incident wave height range for 3 water depths (20 cm, 25 cm, and 30 cm).

Table 5.3: Average Reflection coefficient, C_r , and D/d ratio for 3 water depths.

Table 5.4: Range of loss coefficient, C_l for 3 water depths.

Table 5.5: Range of C_r values and D/d for three water depths.

Table 5.6: Range of C_r values and D/d for three water depths.

Table 5.7: Range of reflection coefficients and D/d ratio.

Table 5.8: Range of transmission coefficients.

Table 5.9: Range of loss coefficients.

Table 5.10: Determination of wavelength, L for 20 cm water depth.

Table 5.11: Determination of wavelength, L for 25 cm water depth.

Table 5.12: Determination of wavelength, L for 30 cm water depth.

Table 5.13: D/d ratio and W/d ratio

CHAPTER 1

INTRODUCTION

1.1 Background of Study

Breakwater is well known as a structure used to reflect and dissipate the destructive wave energy for the protection of a desired area such as shore and harbour. The breakwater attenuates wave energy through wave breaking, wave overtopping, wave reflection, turbulence, friction, heat, and etc. There are two common types of breakwater; fixed structure and floating structure. Fixed breakwater is a rigid structure that is fixed to the ocean floor. Typical examples of fixed breakwater are rubble mound breakwater and caisson type breakwater. Generally, the wave attenuation performance of fixed breakwaters is greater than floating breakwaters. Fixed breakwaters are capable in suppressing the short waves completely. Hence, they are very often used to provide protection to shore erosion and shipping operations. However, the fixed breakwater construction is relatively expensive and time consuming. Once constructed, the breakwater can hardly be removed. Apart from there, the presence of breakwaters will also change the original near shore current system and cause shore erosion at the down drift of the structure.

As an alternative to fixed structures, floating breakwaters were developed. The floating breakwaters have gained significant interest from recreational harbour, fishing harbour and marinas in recent years due to the basic advantages; flexibility, easy mobilization and installation, and low construction cost.

1.2 Problem Statement

In recent years, floating breakwaters have widely used to protect marinas and recreational lagoon from wind and ship-generated waves without obstructing the aesthetic view of the ocean. The advantages of this structures compared to the conventional fixed breakwaters are economy, mobility, aesthetic, environment-friendly, less interference for sediment transport, short construction time, and it is applicable for poor foundation area.

Previous researchers have studied and evaluated performance of various types of floating breakwaters. Each type of floating breakwater has its unique way in reducing the incident wave energy. Even though there are various commercialized floating breakwaters available in the worldwide market, they are still considerably costly. This is due to exorbitant transportation cost and currency exchange. The long term implications are we will constantly relying on foreign technology, which is a loss to the country.

Therefore, there is a need to develop a local floating breakwater system to alleviate the continuous dependence on foreign products. In order to meet the demand, a group of students from Universiti Teknologi PETRONAS has invented Wave Suppress System (WSS), a solid floating breakwater which is a promising technology for our country that will protect shore area from destructive wave. The WSS is capable of attenuating short period wave height up to 84%. Due to its effectiveness, the invention has received award in Engineering Invention 'N' Innovation Competition 2005 (EINIC) and silver award in International Invention, Innovation, Industrial Design and Technology Exhibition 2005 (ITEX).

The basic advantages of WSS are as follows:

1. Simple

Basic shape is applied in the design (rectangular shape) for the ease of fabrication.

2. Flexibility of placement

WSS can be placed according to the wave current direction and suitable for poor seabed condition.

3. Aesthetics

WSS does not block the view of the sea because the crown of the structure is located near to water surface.

4. Environment-friendly

WSS provide less interference to the sea water circulation and sediment transport.

5. Adaptable to water level change

Due to its floating ability, WSS can adapt to various water level and economical for deep water.

There are also few drawbacks of the system. The disadvantages of WSS are:

1. WSS is only effective in short wave period. For a relatively long wave period, the performance is not very encouraging.
2. WSS has high absorption of water due to the material used. Therefore, WSS has been coated with impermeable membrane; fibre glass which is an additional cost.

The solution for the above problems is to develop an improved WSS that will maximize the wave dissipation features in the product. The improved system is also expected to have better attenuation performance.

1.3 Significance of the Study

The destructive nature of waves has opened the minds of the coastal and ocean engineers to preserve beautiful shore areas from damage, as well as to protect lives and properties near the coast area. Because of cost and aesthetic considerations, there are increased demands of floating breakwater used to resolve strong wave problems especially in small parts of marinas. Even though there are various types of floating breakwaters had been proposed, tested, and commercialised, they are still be bound to some limitations.

The increasing development of marinas and recreational lagoons in Malaysia in recent years has made the need of studying the floating breakwaters more significant. Surprisingly, the existing floating breakwaters available in Malaysia are entirely imported from other countries, particularly US and Europe countries. One of the factors may contributed is the lack of local resources on the development of floating breakwaters. Relying on the foreign technologies will certainly bring more harm than goods to the growth of our country. Therefore, the author made an effective effort to turn the concept of having local made floating breakwater into reality and at the same time, protects our own heritage.

1.4 Objective of the Study

For this project, the objectives of the study are as follows:

1. To modify the existing design of Wave Suppress System for the enhancement of the wave attenuation performance.
2. To determine the attenuation characteristics of the wave for different wave conditions and model arrangements via laboratory experiment.
3. To compare the wave attenuation performance of newly proposed design with the existing results by other researchers and inventors.

1.5 Scope of Study

In order to achieve the objectives, the study has been divided into 5 major elements as follows:

1. Literature Review

The existing floating breakwater designs developed by other researchers have been referred and wave dissipation mechanisms inherited from various types of floating breakwaters are studied thoroughly.

2. Development of New Design

The design feature of the existing Wave Suppress System is modified with the aim to enhance its wave attenuation performance in wave field.

3. Laboratory Set Up

Operation of the wave flume must be familiarized prior to the experiments to avoid malfunctioning of the system. Apparatus and equipments used for the experiments are checked for the accuracy of the experimental results obtained.

4. Experiments

Experiments are conducted in wave flume for acquiring the coefficients of transmission, reflection and energy loss of the newly proposed floating breakwater system.

5. Analysis of Results

Results from series of experiment are analyzed and interpreted. An attempt is also made to compare the results with those presented by other floating breakwaters design.

CHAPTER 2

LITERATURE REVIEW

2.1 Wave Breaking, Wave Run-up, and Wave Overtopping

Breaking occurs when the increase in wave steepness due to shoaling and refraction exceeds a limiting value. Typically, breaking occurs when the water depth is about equal to the wave height. Breaking is one of the main mechanisms for the dissipation of wave energy and is responsible for much of the sand movement within the surf zone. Breaking waves impose much higher forces on structures than equivalent non-breaking waves. Depending upon wave characteristics and the slope of the near shore seabed, waves break in either a "surging", "spilling" or "plunging" mode, the difference in these types being visually quite obvious.

When breaking wave approach a structure, the vertical distance between the maximum height the water runs up the structure and the still water level is called wave run-up. Wave run-up is considerably reduced if the structure or beach is rough or porous. The run-up height is reduced when waves approach the structure at an angle.

If the wave run-up is sufficiently high, the wave crest will rise above the crest elevation of the structure, thus produce wave overtopping. For economic, aesthetic and functional design consideration, wave overtopping could be allowed because lower structure is cost effective and will not block the ocean view. If the structure is a breakwater or jetty with water in the lee side, wave transmission will result.

2.2 Wave Reflection

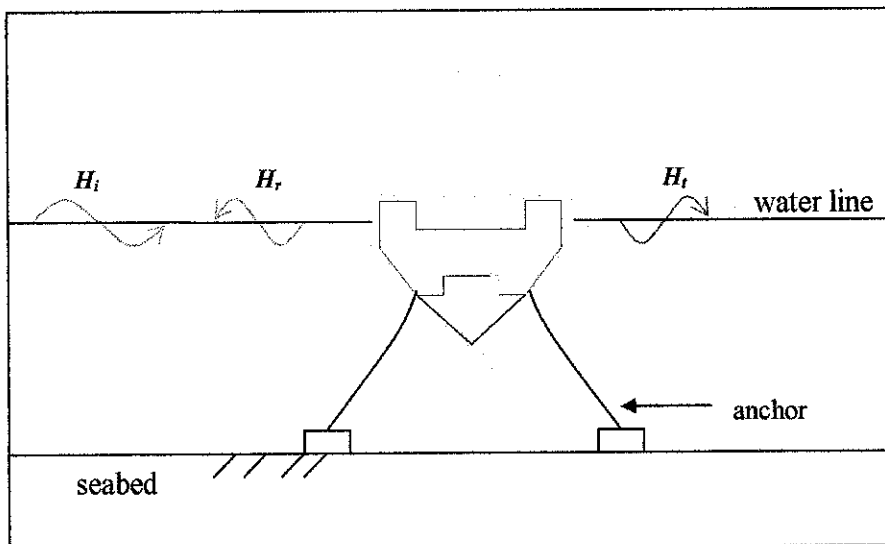


Figure 2.1: Types of wave height; incident wave height (H_i), reflected wave height (H_r), and transmitted wave height (H_t).

Reflection refers to the re-direction by the shoreline of non-dissipated wave energy back to sea. Reflection is most apparent at solid seawalls where reflected waves can be seen moving seawards, virtually unaffected by incoming waves. The wave motion in front of reflecting structure is mainly determined by reflection coefficient, C_r ,

$$C_r = \frac{H_r}{H_i} \quad (2.1)$$

where H_r is reflected wave height and H_i is the incident wave height as illustrated in Figure 2.1. If 100% of wave energy is reflected (total reflection), the C_r is equal to 1. This is generally valid for impermeable vertical wall of infinite height. The reflection coefficient for sloping, rough or permeable structures are smaller.

2.3 Wave Transmission

The effectiveness of a breakwater in attenuating wave energy can be measured by the amount of wave energy that is transmitted past the structure. The greater the wave transmission coefficient, the less the wave attenuation performance. Wave transmission is quantified by the use of the wave transmission coefficient, C_t

$$C_t = \frac{H_t}{H_i} \quad (2.2)$$

where H_t is the height of the transmitted wave on the landward side of the structure as illustrated in Figure 2.1, and H_i is the height of the incident wave on the seaward side of the structure.

2.4 Energy Loss

When a wave hits on a floating structure, some of the wave energy is reflected to the lee of the structure; some energy is used to excite the structure in motions; some is transmitted to the lee of the structure and form a new wave. The remaining energy lost through the wave dissipation mechanisms as follows:

1. Wave breaking on the structure.
2. Turbulence due to the structure feature.
3. Transformation of energy into sound, heat, etc.

For a typical flow, the energy loss of the system can be represented by

$$E_i = E_r + E_t + E_l \quad (2.3)$$

where E_i is incident wave energy, E_r is reflected wave energy, E_t is transmitted wave energy, and E_l is energy loss. In other terms,

$$\frac{(\rho g H)^2_i}{8} = \frac{(\rho g H)^2_r}{8} + \frac{(\rho g H)^2_t}{8} + \frac{(\rho g H)^2_l}{8} \quad (2.4)$$

The equation above can be simplified as,

$$H_i^2 = H_r^2 + H_t^2 + H_l^2 \quad (2.5)$$

By dividing the incident wave heights at the both terms, it yields

$$1 = C_r^2 + C_t^2 + C_l^2 \quad (2.6)$$

where C_r is reflection coefficient, C_t is transmission coefficient, and C_l is loss coefficient.

Rearranging Equation (2.6),

$$C_l = \sqrt{1 - (C_t)^2 - (C_r)^2} \quad (2.7)$$

2.5 Performance of Existing Floating Breakwater

Various existing floating breakwaters have been studied for the development of improved IWSS. Some of the floating breakwaters and its performance are discussed in this section as follows.

2.5.1 Various Floating Breakwaters Configurations

Blumberg and Cox (1988) and Wright (1989) had tested sixteen separate floating breakwaters configurations, covering prototype wave climates ranging from 1.5 to 5 seconds and 0.2 to 1.2 m height. Model 1 to 6 is different combinations of commercially available rectangular prism as illustrated in Figure 2.2; Model 7 to 11 is different rectangular prism in catamaran configurations as illustrated in Figure 2.3; and Model 12 to 16 is catamaran floating breakwaters incorporating curved keels and slatted keels as illustrated in Figure 2.4.

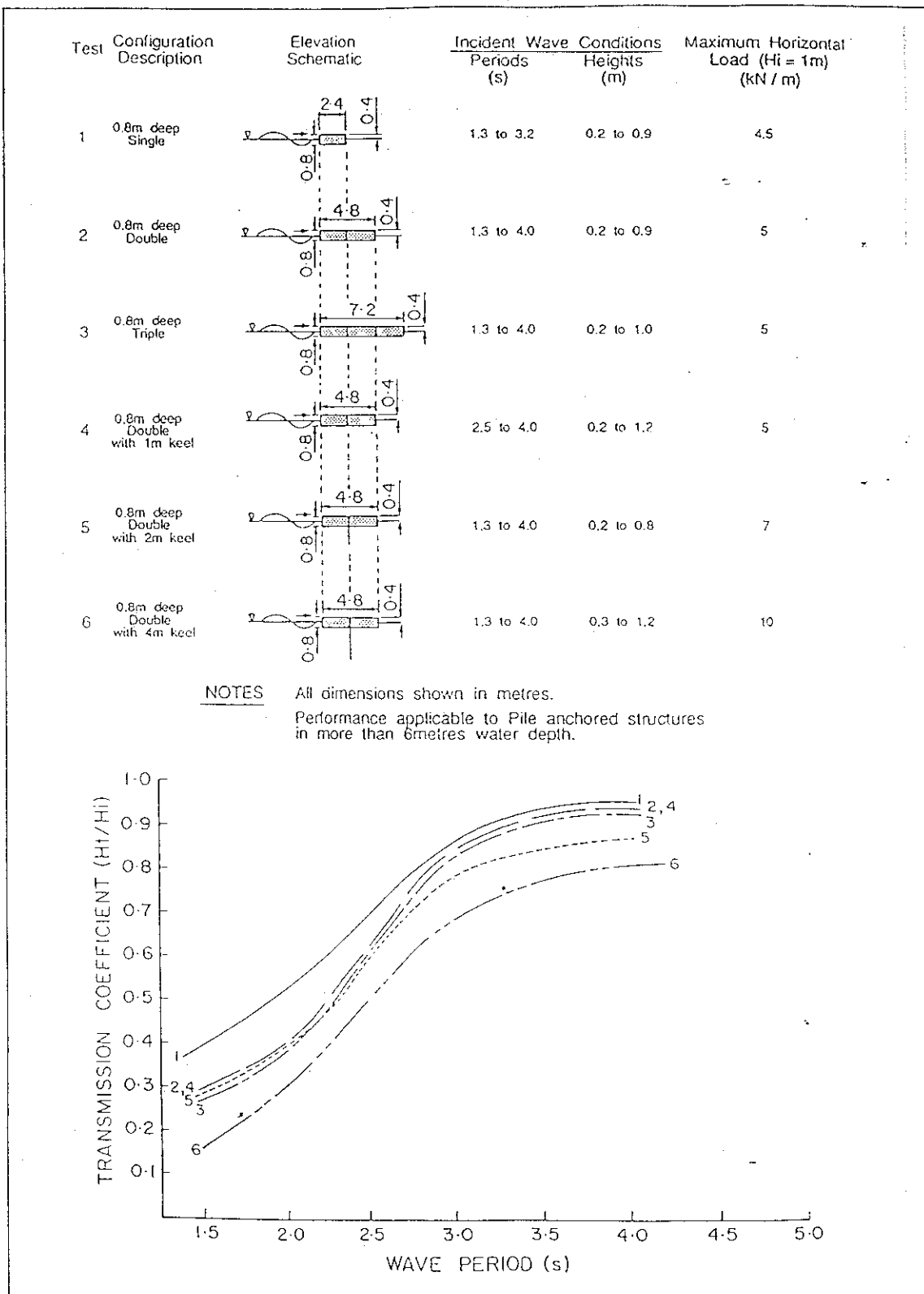


Figure 2.2: Model 1 to 6 and its transmission coefficients. (Source: COPEDEC III – Third International Conference on Coastal and Port Engineering in Developing Countries Mombassa, Kenya)

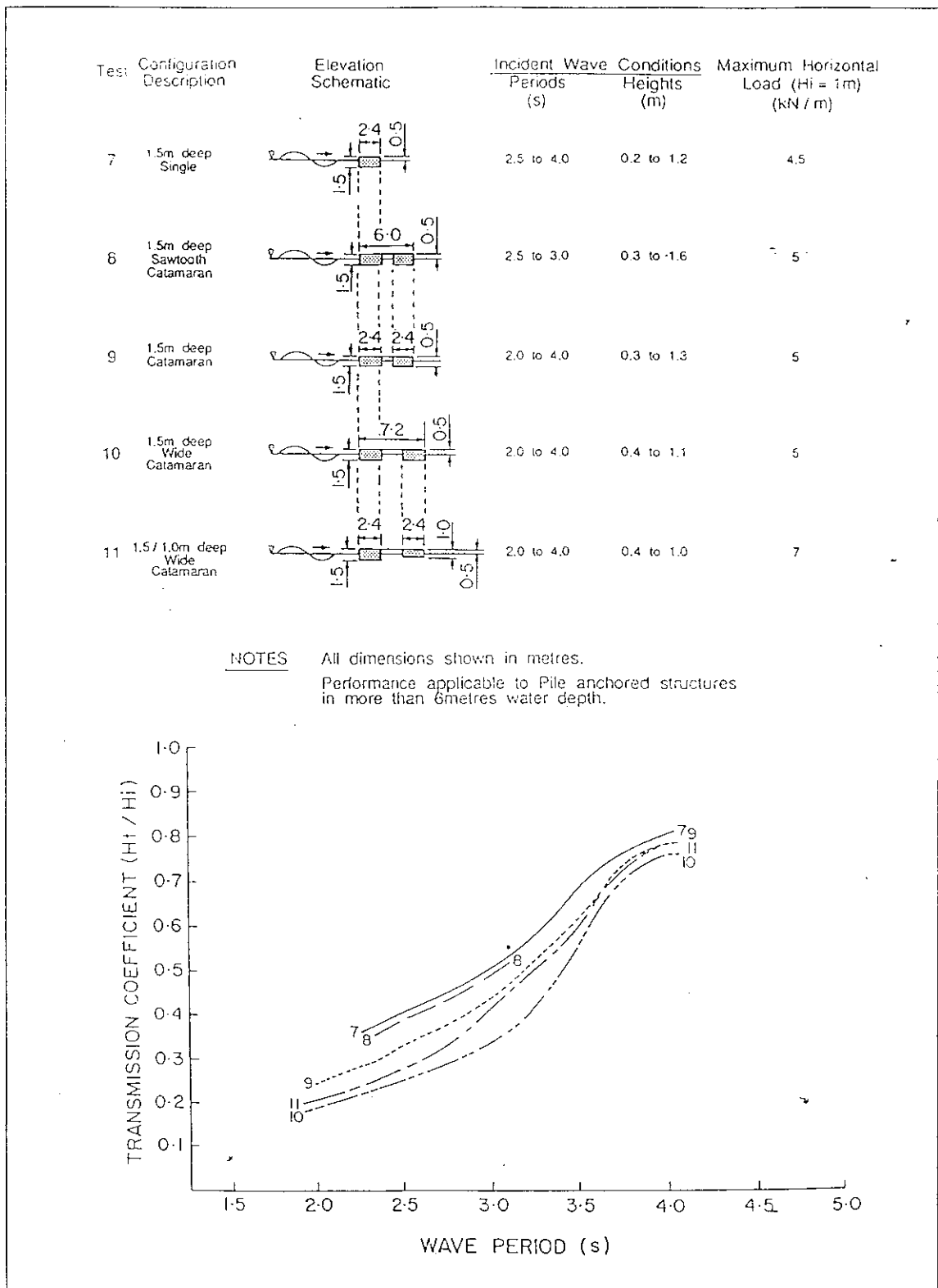


Figure 2.3: Model 7 to 11 and its transmission coefficients. (Source: COPEDEC III – Third International Conference on Coastal and Port Engineering in Developing Countries Mombassa, Kenya)

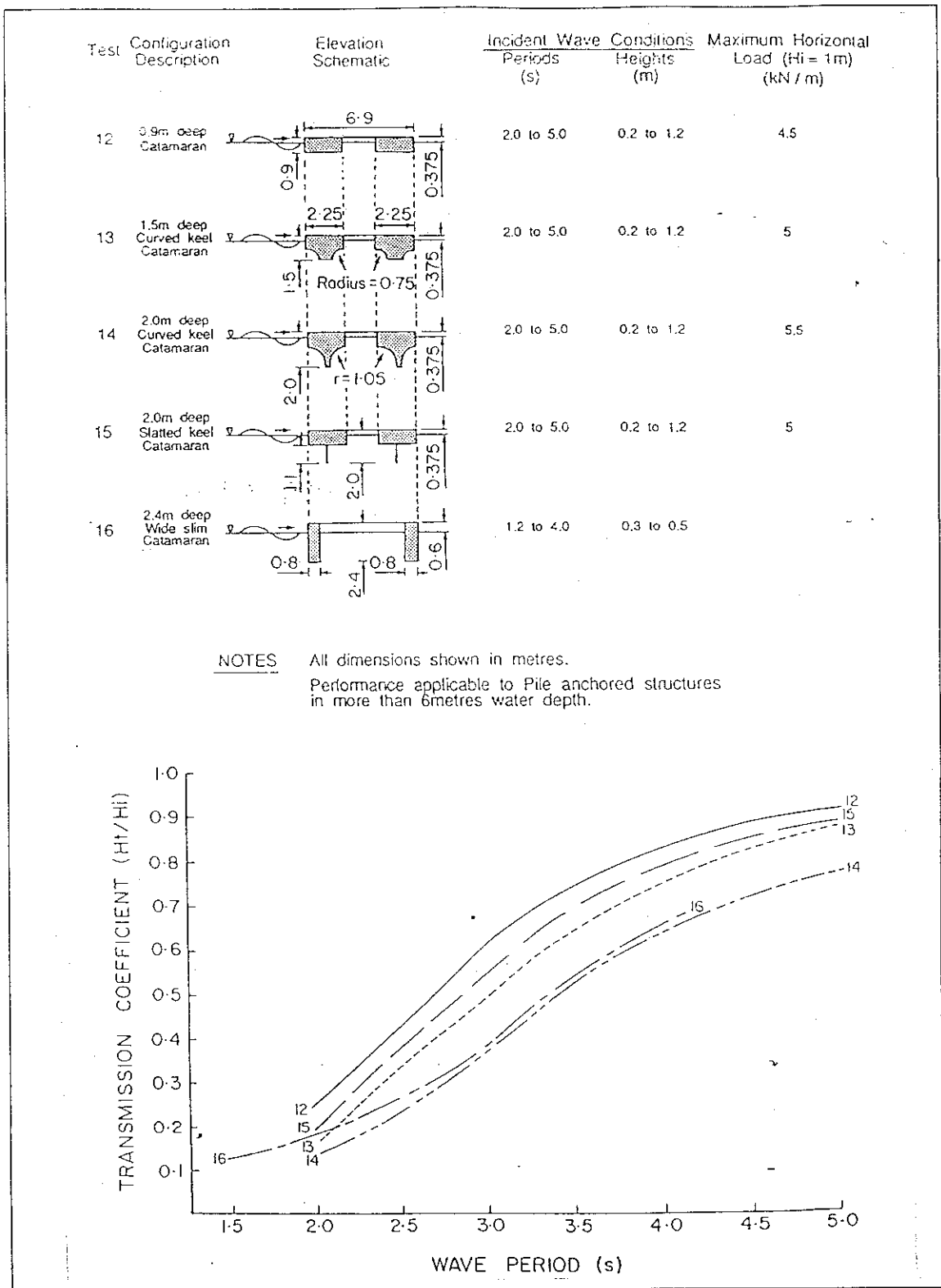


Figure 2.4: Model 12 to 16 and its transmission coefficients. (Source: COPEDEC III – Third International Conference on Coastal and Port Engineering in Developing Countries Mombassa, Kenya)

The results are presented in terms of transmission coefficients and wave period. From Figure 2.2, it is clear that attenuation performance is improved with increasing width of the structure. It is also shown that attenuation performance is improved by increasing the depth of the centreboard keel.

Figure 2.3 shows that the continuous catamaran (Model 9) has a better wave attenuation performance sawtooth catamaran (Model 8) of the same width. It is clearly shown that Model 10 has better attenuation performance for rectangular prism in catamaran configurations. Rectangular prism in catamaran configurations performance is more encouraging than rectangular prism in Figure 2.2.

Figure 2.4 shows that Model 14 gives the best attenuation performance followed by Model 16, Model 13, Model 15 and Model 12. It is worthwhile to note that ever through the floating modules of Model 12 and Model 15 are same configurations. However, Model 15 provides a better performance due to the attachment of slatted keel below the structure. Model 13 has better attenuation performance than Model 15 due to the increased mass by 30%. Attenuation performance of Model 14 compared to Model 13 shows significant improvement due to additional 0.5 m draft, increase in mass of 15% and an increase in hull curvature.

It is clearly noted that curved catamarans have better attenuation performance than rectangular prism catamaran and rectangular prism. However, the curvature models are very costly as compared to rectangular shape models due to additional materials required for fabrication. For the conclusion, curved keel catamaran designs shown to have the best wave attenuation performance while slatted keel catamaran designs have most cost efficient performance.

2.5.2 Cage Floating Breakwater (CFB)

Murali and Mani (1991) has developed cage floating breakwater to meet the demand of cost effective floating breakwater. The design has been referred from Y-frame floating breakwater (Mani 1991). The CFB consists of two trapezoidal pontoons with two rows of closely spaced pipes as illustrated in Figure 2.5. The space between the pontoons

might serve as the cage by enclosing suitable nylon mesh. The row of pipes does not contribute significantly to the buoyancy but acts as an effective barrier to the incident waves.

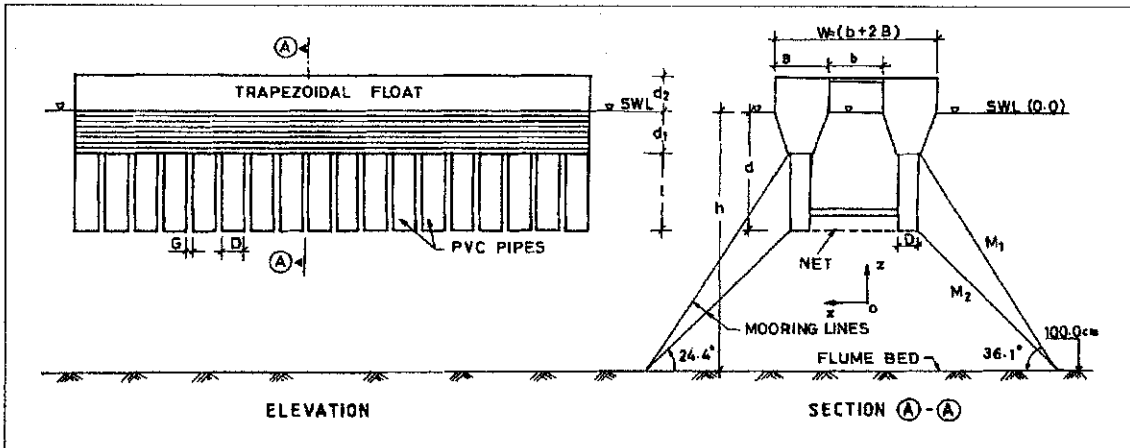


Figure 2.5: Cage floating breakwater. (Murali and Mani, 1997)

The performance of CFB is illustrated in Figure 2.6. The performance is presented in terms of transmission and reflection coefficients with wave steepness parameter, H_1/gT^2 . The figure shows for $H_1/gT^2 > 0.01$, the transmission coefficient is less than 0.1, which means CFB is capable of attenuating more than 90% of wave heights. The variation of reflection coefficients show that C_r increases with an increase in H_1/gT^2 . It should be noted that at $H_1/gT^2 = 0.0038$, C_r is equal to C_t .

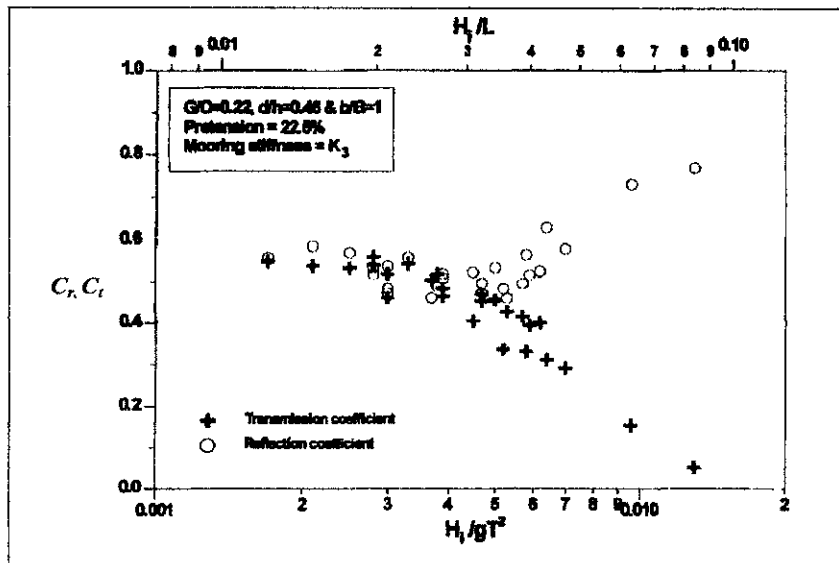


Figure 2.6: Variation of transmission and reflection coefficients.

(Murali and Mani, 1997)

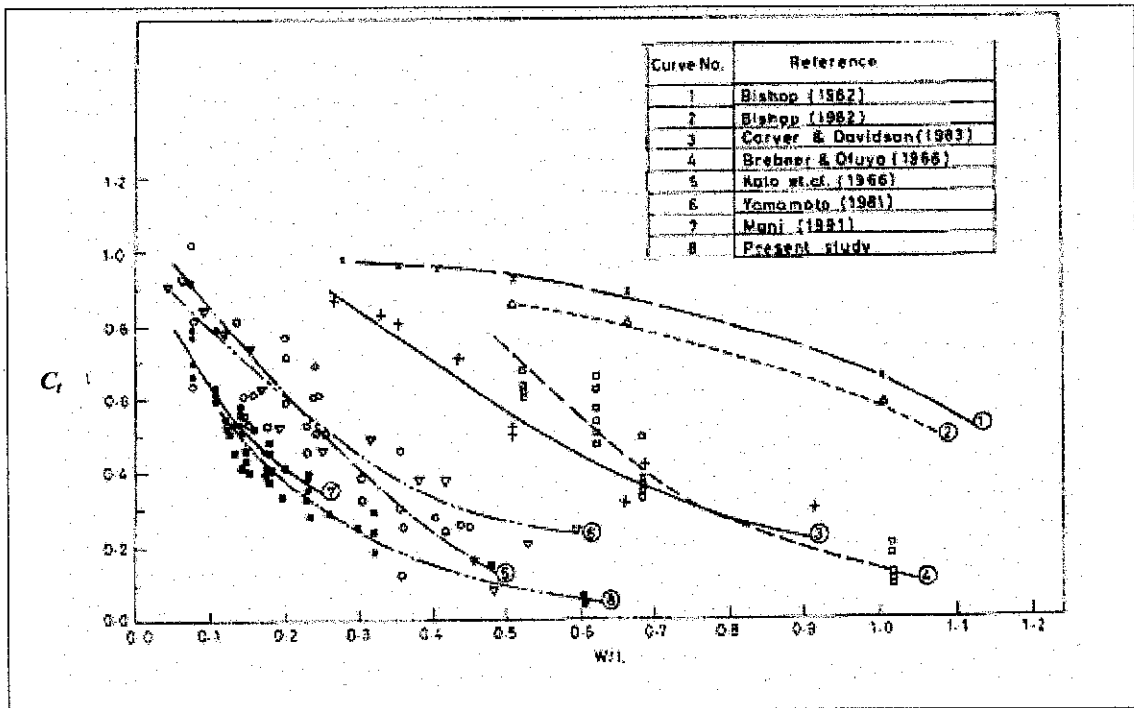


Figure 2.7: Performance of various studies of floating breakwater.

(Murali and Mani, 1997)

Murali and Mani (1991) had also made efforts to compare the performance of CFB with previous similar experimental studies conducted by Kato *et al.* (1966), Brebner and Ofuya (1968), Yamamoto (1981), Bishop (1982), Carver and Davidson (1983), and Mani (1991) as illustrated in Figure 2.7. From Figure 2.7, CFB has the best transmission coefficient as compared to other floating breakwater. For $0.14 < W/L < 0.6$, the CFB would be capable of restricting the transmitted wave height below 50% of incident wave height. The figure also indicates that CFB is more efficient in controlling the transmission coefficient compared to Y-frame floating breakwater.

2.5.3 Freely Floating Porous Box

Freely floating structure with very soft moorings system as illustrated in Figure 2.8 had been studied by Drimer and Stiasnie (1992) to overcome large oscillatory forces in their mooring system. The experiment examined the suitability of freely floating porous structures, which absorb part of wave energy, to serve as breakwater. The experiment had been referred from the study of interaction of waves with fixed porous boxes by Dalrymple *et al.* (1991).

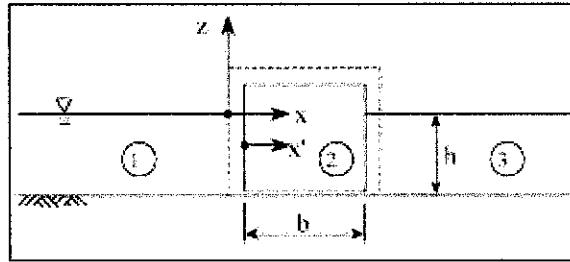


Figure 2.8: Schematic diagram of floating porous box. (Drimer and Stiassnie, 1992)

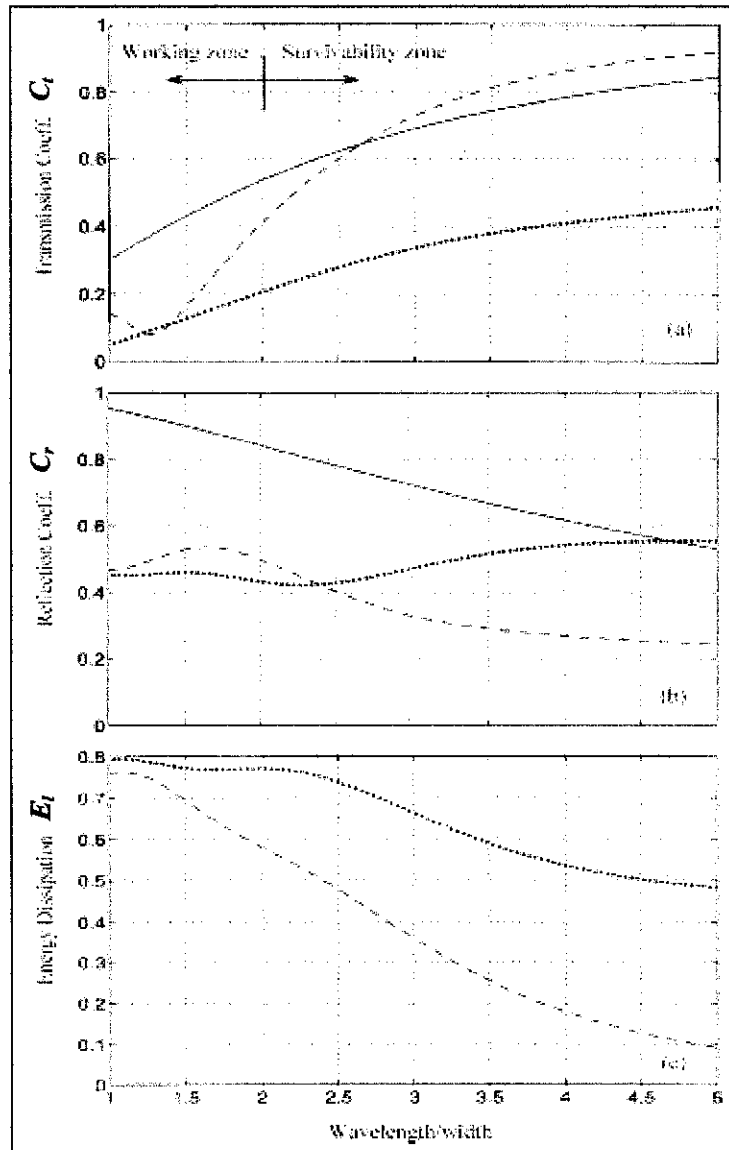


Figure 2.9: Comparison of performance between a porous fixed box (...), a porous free box (---) and an impermeable free box (—). (Drimer and Stiassnie, 1992)

Figure 2.9 shows transmission and reflection coefficients, and energy loss for three different boxes, porous fixed box, porous free box and impermeable free box. For the transmission coefficient, porous free box has better performance than impermeable free box but fixed box is more effective in attenuating the wave energy. Fixed box is considered as a submerged breakwater; hence it has better attenuation performance.

For reflection coefficient, porous free box can reflect relatively small wave energy compared to impermeable box because the waves pass through the porous medium rather than reflected back to the seaward. Energy dissipation indicates that more than half of the wave energy is dissipated by free porous box in its working zone, compared to fixed porous structure. Therefore, it can be concluded that free porous box is capable of dissipating more than half of wave energy compared to fixed box.

2.5.4 Wave Suppress System (WSS)

Wave Suppress System was developed by a group of UTP students for their Engineering Team Project (2004) which is one of the core subjects for all the engineering courses in the university. The WSS is H-shape floating breakwater designed to dissipate wave energy through four main mechanisms; reflection, wave breaking, friction and turbulence. The size of the WSS is 20 cm width (W), 30 cm length (l), and 10 cm height (h) as illustrated in Figure 2.10. It has 3.5 cm freeboard and 6.5 cm draft. The overall density is 650 kg/m^3 and the material used is Autoclaved Lightweight Concrete (ALC) with fiberglass coating.

Figure 2.11 shows the wave attenuation performance of WSS in terms of wave transmission coefficient, C_t and width-to-wavelength ratio. The graph shows C_t decreases with the increasing W/L . It can be seen from the graph that there is a sudden drop in C_t value as W/L increases from 0.05 to 0.20. It indicates that WSS is less effective in dampening the longer waves in the flume. It is further observed from the graph that the WSS is capable to attenuate 90% of the incident wave height when W/L is approaching 0.4. This indicates that WSS can perform at it best in short-length waves or short wave period.

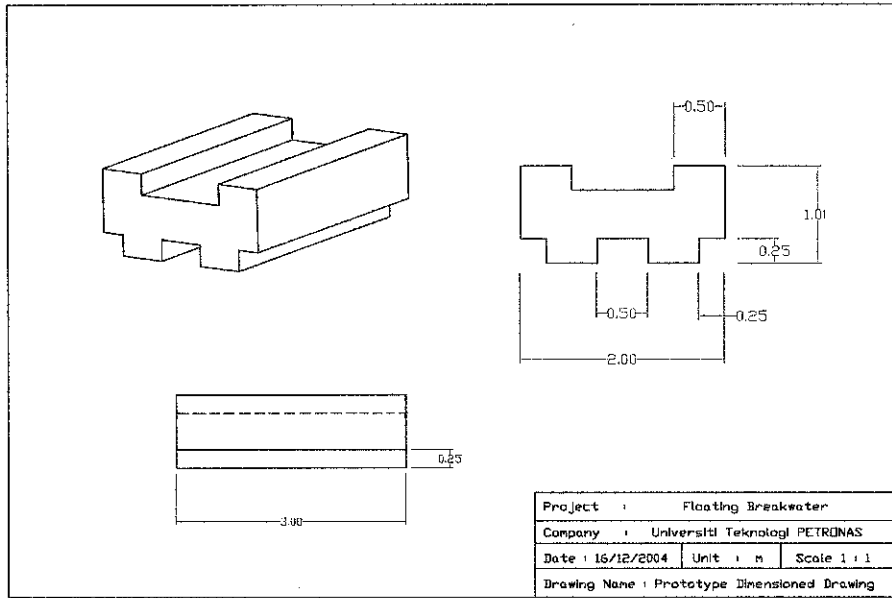


Figure 2.10: Wave Suppress System.

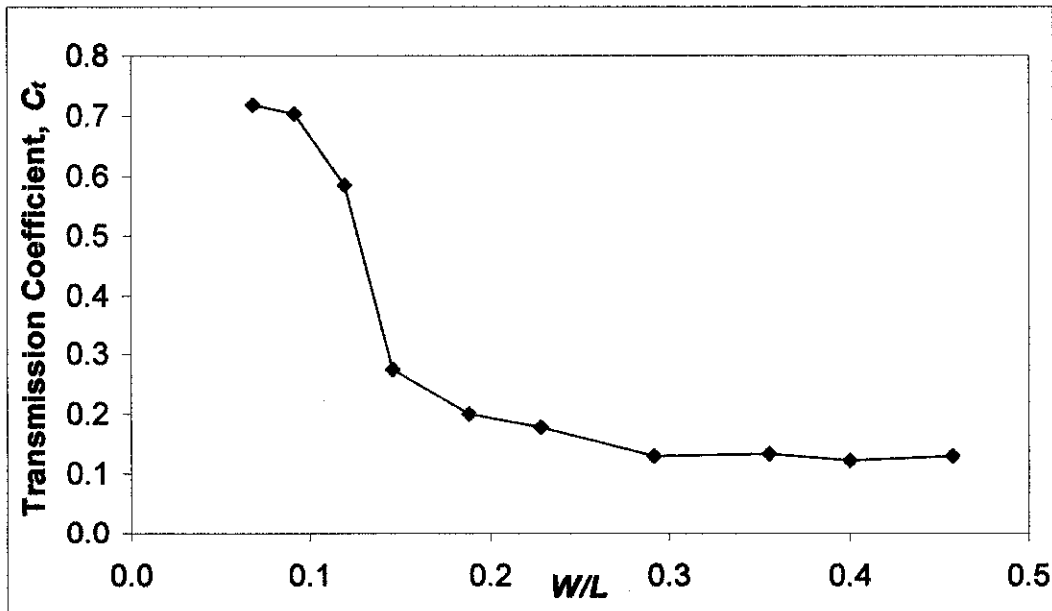


Figure 2.11: Transmission coefficient of WSS.

However, the experiment was conducted in a limited wave range in the flume. The WSS has been tested in 30 cm water depth for wave period ranging from 0.5 to 1.4 seconds only. It is recommended that the model should be tested in greater range of wave conditions so that the results yields are more comprehensive.

2.5.5 Comparison of Existing Breakwaters Performance

The performance of existing floating breakwaters in term of transmission coefficient and ratio of width over wavelength is illustrated in Figure 2.12. From the figure, all curves show similar trend and shape. The curves also show that C_t value decreases as W/L increases.

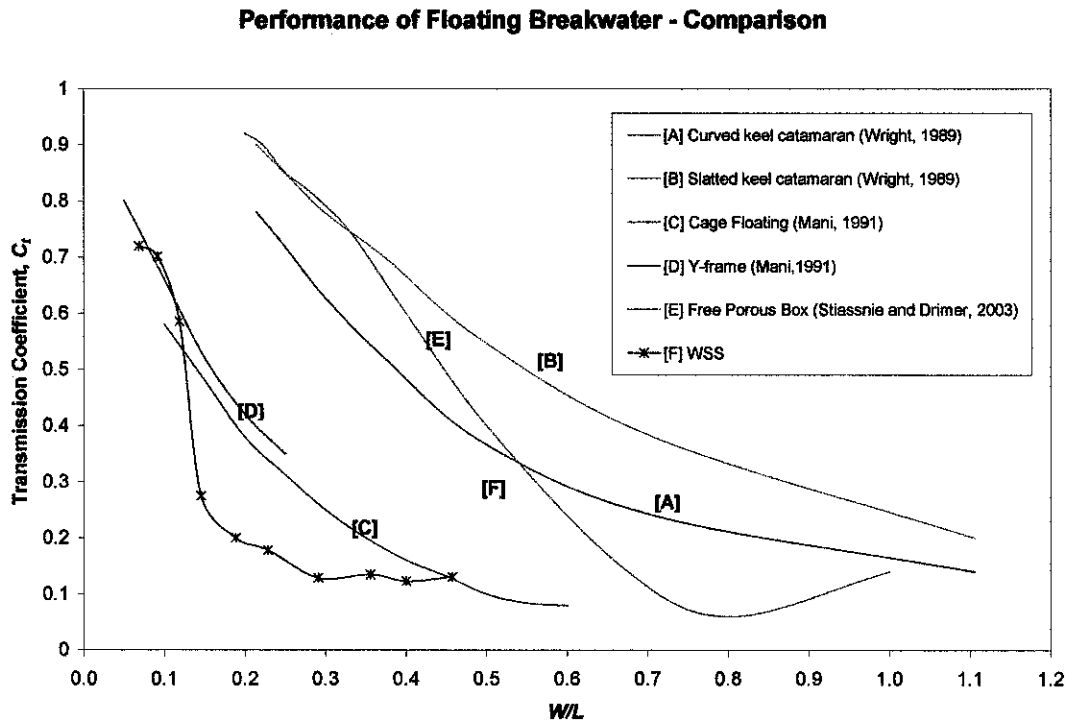


Figure 2.12: Comparison of Floating Breakwater Performance.

From Figure 2.12, we can see that there are two groups of curves that have resulted in similar shape, which are a) curve [A] and curve [B], and b) curve [C] and curve [D]. Curve [A] and curve [B] is the comparison between curved and slatted keel catamaran by Wright (1989), which indicates that curved catamaran performs better but cost higher than slatted catamaran. For curve [C] and curve [D], Mani (1991) has studied that Cage Floating Breakwater is 10-20% more efficient than Y-frame Breakwater.

Free Porous Box and Cage Floating Breakwater have shown remarkable performance as both is capable attenuating wave heights more than 90% due to high ratio of width-to-depth which is 5. Wave Suppress System shows reasonably good wave

attenuation performance with respect to other floating breakwaters. Therefore, further improvement of WSS design is essential to enhance the wave attenuation ability.

2.6 Floating Breakwater Design Criteria

Normally, two general physical principles can be used to explain the wave attenuating ability of a specific floating breakwater are **reflection** and **turbulence**.

The best reflectors are probably bulkheads. When a wave hits a flat shoreline bulkhead, it is almost entirely reflected. For reflective-type floating breakwaters to be effective, rigidity of the breakwater in the water is the key characteristic required to stop waves. If the breakwater is able to move significantly in the water, the wave attenuation capabilities of that reflective surface are greatly reduced. Another characteristic required for effective operation of a reflective-type breakwater is draft. Without sufficient draft, much of the wave energy will pass below the breakwater and will rebuild waves on the lee of the breakwater.

For turbulence-type breakwaters, low draft and generally large width with respect to the wave size could produce most effective attenuation performance. The width of a turbulence-type breakwater should generally be at least equal to 1.0 to 1.5 times the wave length of the design wave. It is normally not necessary for a turbulence-generating breakwater to be rigid, and in fact, most breakwaters are characterized by the flexibility of the entire breakwater system. Another form of wave turbulence attenuation is caused by friction during the movement of water along the bottom of a large flat plate. This is how a large flat raft, which is rigid and very wide with respect to design wave, can be used to stop waves.

CHAPTER 3

IMPROVED WAVE SUPPRESS SYSTEM (IWSS)

3.1 Introduction

The study of floating breakwater performance has received significant attention due to the advantages that floating breakwaters could offer compared to fixed breakwaters. Through extensive literature review on the existing type of breakwaters, the general design criteria of efficient floating breakwaters had been identified and applied in the Improved Wave Suppress System (IWSS). The aim of the design is to produce an efficient floating wave attenuator as well as a cost effective structure.

3.2 Development of IWSS

The existing design of Wave Suppress System (WSS) was referred for the development of the present design (IWSS). The IWSS is targeted to have better performance compared to WSS in attenuating wave energy by making few modifications on the design of WSS.

3.3 Description of IWSS

Figure 3.1 shows the cross sectional area of the IWSS model and Figure 3.2 shows the isometric view and side view of IWSS. Each floating module has 30 cm length (l), 20 cm width (W) and 10 cm height (h). There are also two keel plates attached to the bottom of the structure for greater stability in the wave field.

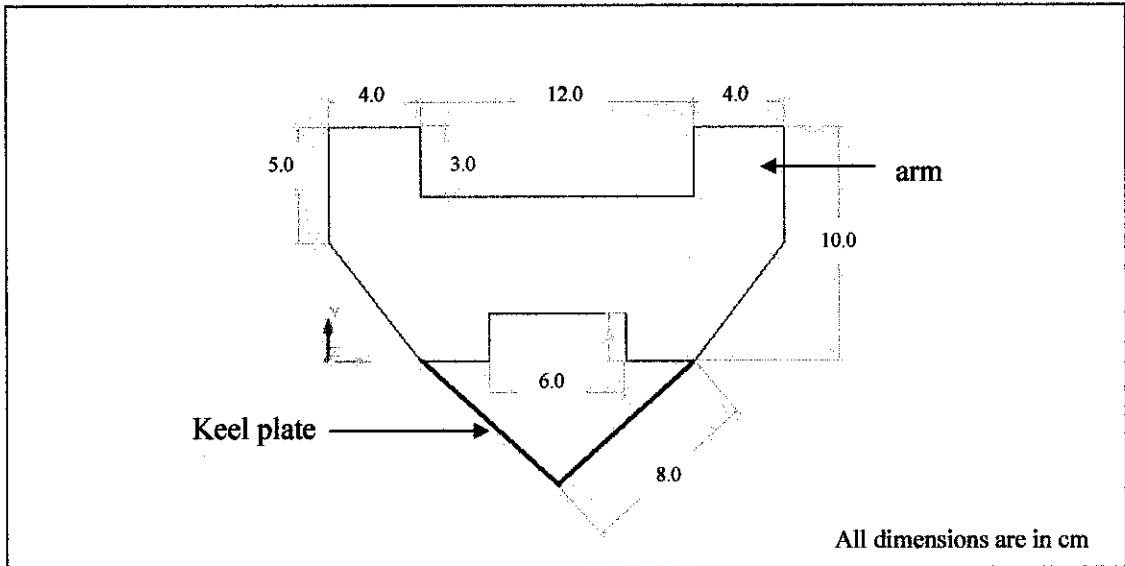


Figure 3.1: Cross section of IWSS.

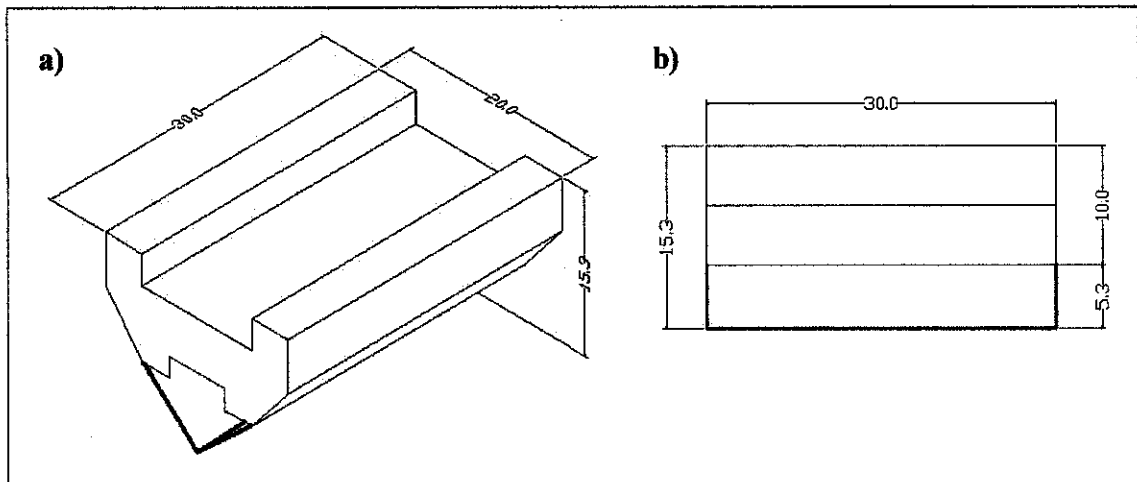


Figure 3.2: a) Isometric view and b) side view of IWSS.

The materials used for the models of IWSS are Autoclaved Lightweight Concrete (ALC), water proofing membrane and stainless zinc sheet as illustrated in Plate 3.1 and Plate 3.2. ALC is a mix of sand, lime and cement together with a gas-forming agent. ALC has 500 kg/m^3 dry density. Table 3.1 indicates the nominal properties of the ALC used for fabricating the models.

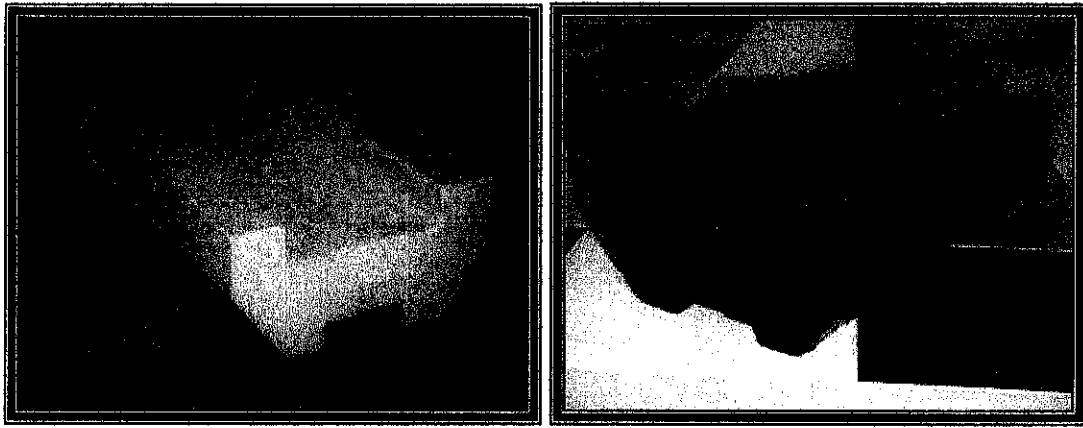


Plate 3.1: Model of IWSS before and after painted with water proofing membrane.

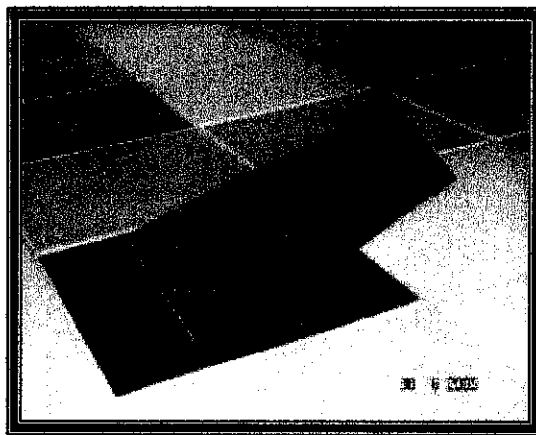


Plate 3.2: Keel plate.

For the surface hardness, ALC is repaired to be 70% better than conventional concrete. ALC is been chosen for the model fabrication of IWSS due to its lower density compared to normal concrete for greater floatability.

The only drawback of using ALC is that it has seven times higher total porosity than the normal weight concrete. Therefore, the model needs to be coated with water proofing membrane, which is a membrane that is painted to the model to avoid seepage of water into the model, thus preventing from submergence of the models into the water.

For the keel, stainless zinc plates with 1 mm thickness are applied to prevent the structure from corrosion. The calculation for buoyancy force, mass, and density of IWSS in static condition is shown in the Appendix 2.

Table 3.1: Nominal properties of Autoclaved Lightweight Concrete.

Properties	Value
Compressive Strength, f_{cu}	2.8 MPa
Minimum Compressive Strength, f_m	2.5 MPa
Modulus of Elasticity, E	1500 MPa
Modulus of Rupture, f_{ut}	0.44 MPa
Ultimate Tensile Strength, f_{mt}	0.44 MPa

3.4 Conceptual Wave Dissipation Mechanism of IWSS

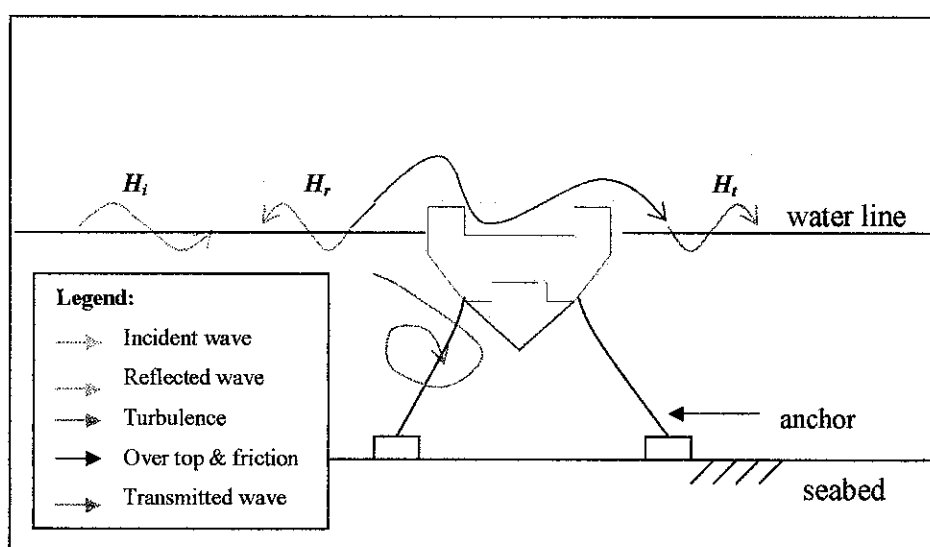


Figure 3.3: Wave dissipation mechanism of IWSS.

The primary mechanisms of energy dissipation of the improved design are wave reflection, turbulence, wave absorption, wave over topping and friction as illustrated in Figure 3.3. When a wave approaches the structure, the vertical seaward side of the structure will reflect the wave energy back to the sea. Some of the wave energy which travels underneath of the structure is dissipated to certain extent due to turbulence between the keels. It is believed that the presence of keel plates underneath the floating structure would further increase the wave damping characteristics of IWSS. Some of the wave energy is directed to the further downwards and get dissipated, and some will pass through those holes on the seaward keel plate, producing an expansion current and turbulence within the entrapped space in which it may reduce the wave energy.

For waves that overtop the structure, most waves will break at the seaward arm of the structure and the remaining energy will be dissipated by friction between the wave and the rough surface of the structure. There will be some waves, which have not been dissipated through the above mentioned mechanisms, transmit to the leeward side of the structure and create a new form of wave with a dampened height.

CHAPTER 4

EXPERIMENTAL SET UP AND PROCEDURE

4.1 Introduction

A comprehensive model testing was conducted in the laboratory to monitor the performance of IWSS. The experimental works were carried out in the Coastal and Hydraulics Laboratory of UTP. To obtain quality results, it is essential to be familiarized with the equipment and instrumentation to be used for the experimental purposes. In this chapter, equipment used and procedures in conducting experiments will be explained in detail. The measured parameters that were used to measure the performance of the IWSS are incident wave height (H_i), reflected wave height (H_r), transmitted wave height (H_t), and wave period (T).

4.2 Laboratory Equipment and Instrumentation

The laboratory experiments were conducted in a 10 m long, 30 cm wide, and 45 cm high wave flume as shown in Plate 4.1. It has a rigid steel bed and the sides are lined with glass panels for the entire length of flume for observation of the processes inside the flume. Waves are generated by flap-type wave paddle as shown in Plate 4.2.

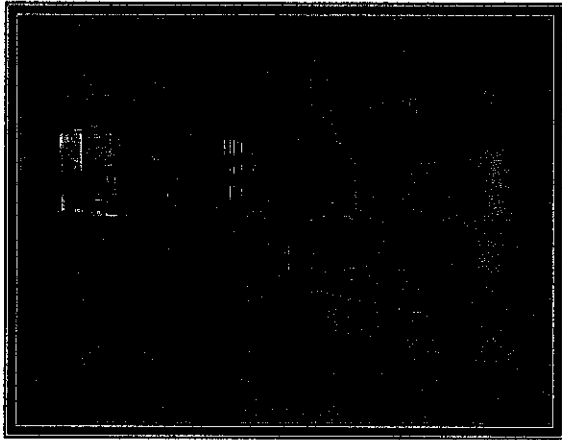


Plate 4.1: Wave flume

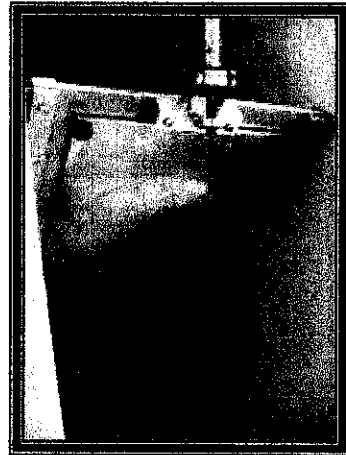


Plate 4.2: Wave paddle

Plate 4.3 shows the wave generator and the switch box. The wave generator is bolted onto the surrounding edge of the wave flume. The wave generator is driven by a gear motor. The rotary movement of the motor is converted into a harmonic stroke motion of the movable paddle via a crank disc with push rod. All electrical switching units required for operations are located in the cover of the switch box. The rotational speed gives the stroke frequency of the wave generator and can be adjusted via a 10-gear helical potentiometer. At 100%, the rotation speed is 114 rpm. With linear characteristic, the rotational speed at 0% is 0 rpm.

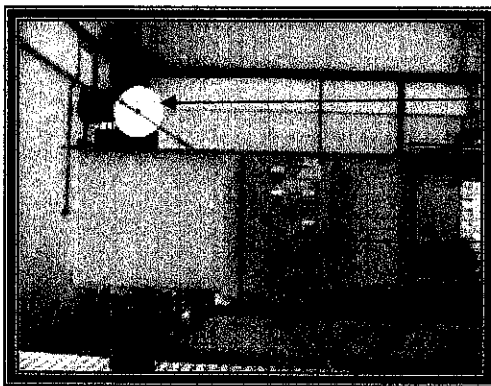


Plate 4.3: Wave generator and switch box.

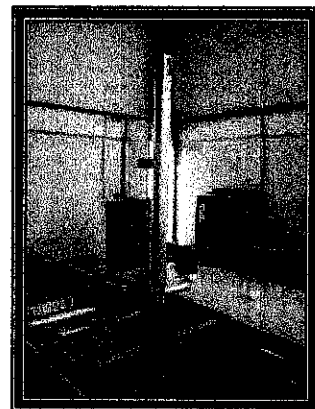


Plate 4.4: Hook and point gauge.

The hook and point gauge shown in Plate 4.4 is used to measure water level in the wave flume. It is possible to carry out measurements over the entire working range of the

flow channel, since the measuring point can be traced in the longitudinal direction, across the width and in depth of the flow channel cross section.

Another equipment that were used in the experiments is wave absorber. Wave absorber is a defence structure located at the reflective boundaries of wave flume to attenuate incoming wave energy through various wave dissipation mechanisms. Plate 4.5 shows the side view of the wave absorber and Plate 4.6 shows the placement of the wave absorber in the wave flume. The wave absorber consists of wire mesh absorber with adjustable slope angle from 0° to 90° . The design calculation is presented in Appendix 1. The size of the wave absorber is 120 cm (length) x 30 cm (width) x 120 cm (slope length). Throughout the experimental studies, angle 15° were used due to its effectiveness in dissipating waves.

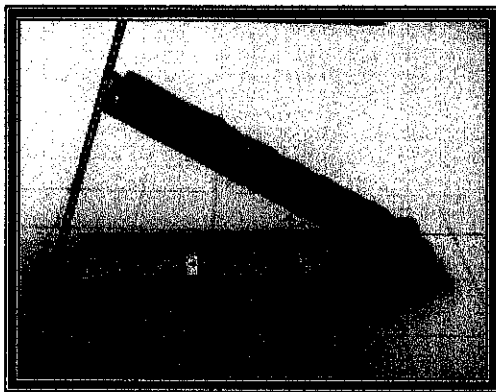


Plate 4.5: Side view of wave absorber.

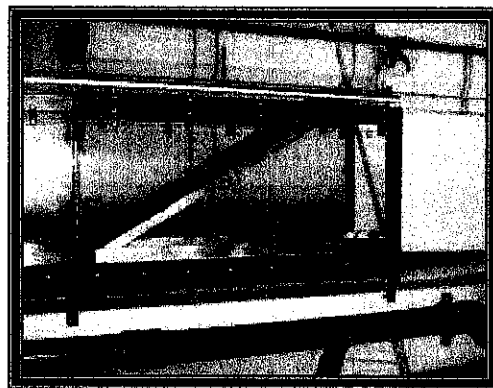


Plate 4.6: Placement of wave absorber in the wave flume.

4.3 Experimental Procedures

Series of experiments were conducted in order to monitor the performance of the IWSS with different wave periods, water depths and stroke adjustments. The purpose is to observe the behaviour of IWSS in various water and wave conditions.

4.3.1 Preliminary Test

The main objectives of the preliminary tests are to measure wave period, T with respect to different stroke frequencies for the calibration purposes and to measure incident wave height, H_i for the analysis of wave attenuation performances.

The first test is to measure wave period by obtaining time taken for the crank disc to revolve 10 cycles. The process has to be repeated at least three times to find the average time. Measurement of wave period continues for a series of stroke frequencies. The measurement of wave periods are conducted in three different stroke adjustments, mainly 80 mm, 140 mm and 200 mm to observe the characteristics of wave period in different stroke adjustments.

The second test are conducted without the presence of WSS to obtain the incident wave height, (H_i) in three water depth, which is 20 cm, 25 cm and 30 cm. The three water depths have been chosen because the maximum water depth to be analyzed before it splash out from the fume is 30 cm; and the total draft for improved WSS is 15 cm, thus 20 cm is the minimum water depth suitable for the analysis.

During each experiment, minimum of five readings of the wave heights should be obtained and tabulated. Assuming there is no reflection from the wave absorber, the average of incident wave height is obtained using the equation (4.1). After that, the experiments will be repeated for the other two stroke adjustments.

$$H_i = \frac{\sum H_i}{n} \quad (4.1)$$

where n = total number of readings.

4.3.2 Experimental Studies on IWSS

For this project, four sets of experiments will be carried out for comparison of WSS with IWSS in three different configurations. The types of experiments that will be carried out are:

1. Existing system (WSS).
2. Improved WSS.
3. Improved WSS with keel plate.

Each set of experiment will be conducted in three water depths, which are 20 cm, 25 cm and 30 cm water depths. The range of wave period is from 0.5 seconds to 3.0 seconds. The experiments will be also conducted in three different stroke adjustments, which are 80 mm, 140 mm and 200 mm. The total number of runs that will be conducted is as follows:

$$\begin{aligned}\text{Total number of runs} &= 3 \text{ types} \times 3 \text{ water depths} \times 3 \text{ stroke adjustments} \times 16 \text{ wave periods} \\ &= \mathbf{432 \text{ runs}}\end{aligned}$$

The parameters that need to be measured are as follows:

1. Maximum and minimum wave height in front of the structure for the calculation of reflected wave height, H_r given by the equation

$$H_r = \frac{H_{\max} - H_{\min}}{2} \quad (4.2)$$

2. Wave heights (5 readings) at the back of the structure for the calculation of transmitted wave height, H_t given by equation

$$H_t = \frac{\Sigma H_t}{5} \quad (4.3)$$

3. After that, Reflection coefficient, Transmission coefficient, Loss coefficient will be calculated using equation 2.1, 2.2 and 2.7.

CHAPTER 5

EXPERIMENTAL RESULTS AND DISCUSSION

5.1 Introduction

The first part is the results for the preliminary tests. The preliminary tests consist of determination of wave period, determination of incident wave height, and performance of WSS which has been conducted in the first semester.

For the second semester, experimental studies on IWSS have been conducted. The experiments started with model IWSS, followed by IWSS with keel (0% and 50% porosity) in three water depths and three stroke adjustments. Results are presented according to Reflection Coefficient, Transmission Coefficient, and Loss Coefficient. Comparison of each system is made according to water depth; 20 cm, 25 cm, and 30 cm.

5.2 Determination of Wave Period, T

Wave period is time for a successive wave to pass a point. In the laboratory, average time taken for one complete cycle of the crank disc is recorded for a set of stroke frequencies in three different stroke adjustments for calibration purposes. Observed wave period is tabulated in Table 5.1.

The relationship between stroke frequency and observed wave period has been graphically illustrated in Figure 5.1. From the figure, it is noticed that the average observed wave period for the three stroke adjustments most likely the same. This indicates that the wave period does not depend on the stroke adjustment, but only depends on stroke frequency. Figure 5.1 also shows that observed wave period decreases exponentially as the stroke frequency increases. The relationship is expressed by the equation

$$T = 152.52 f^{-1.2362} \quad (5.1)$$

where T = wave period (s) and f = stroke frequency (rpm)

Table 5.1: Observed wave period for 80 mm, 140 mm, and 200 mm stroke adjustment.

Stroke frequency (rpm)	Stroke duration (s/rev)	Observed wave period, T (s)			Average observed wave period, T (s)
		80 mm stroke adjustment	140mm stroke adjustment	200mm stroke adjustment	
108	0.56	0.50	0.47	0.50	0.49
88	0.68	0.64	0.61	0.61	0.62
74	0.81	0.75	0.74	0.75	0.75
64	0.94	0.89	0.87	0.89	0.88
56	1.07	1.04	1.03	1.05	1.04
50	1.20	1.15	1.18	1.21	1.18
44	1.36	1.37	1.36	1.38	1.37
40	1.50	1.55	1.52	1.56	1.54
37	1.62	1.70	1.68	1.73	1.71
34	1.76	1.90	1.88	1.92	1.90
31	1.94	2.14	2.10	2.17	2.14
29	2.07	2.34	2.38	2.40	2.37
27	2.22	2.58	2.64	2.65	2.63
25	2.40	2.88	2.95	2.94	2.92
24	2.50	3.07	3.13	3.11	3.11
23	2.61	3.27	3.34	3.37	3.32

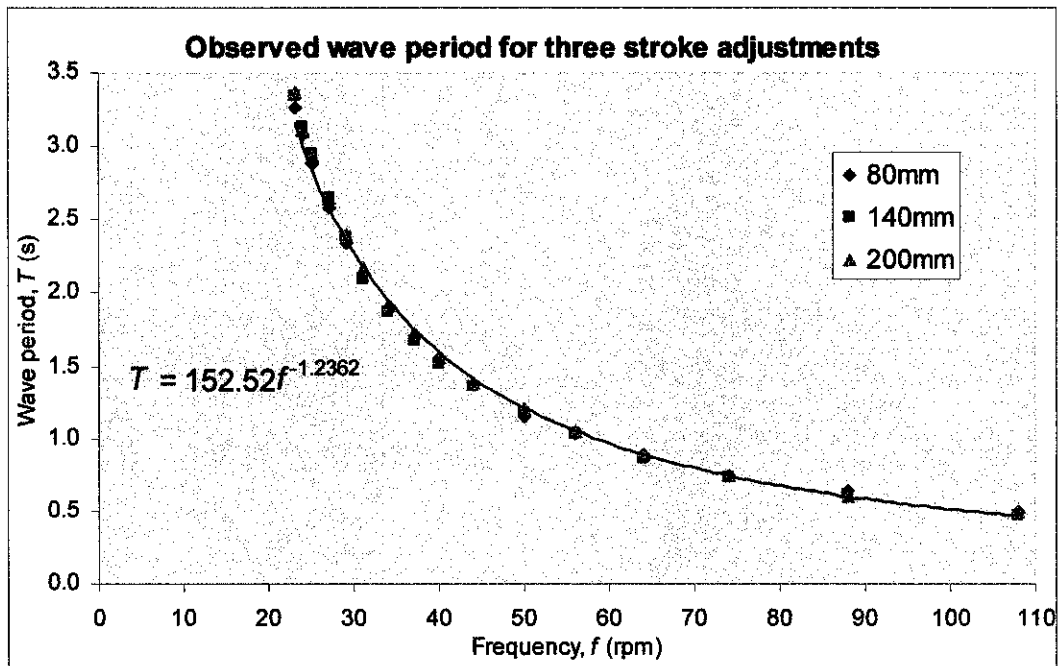


Figure 5.1: Observed wave period for 80 mm, 140 mm, and 200 mm stroke adjustments.

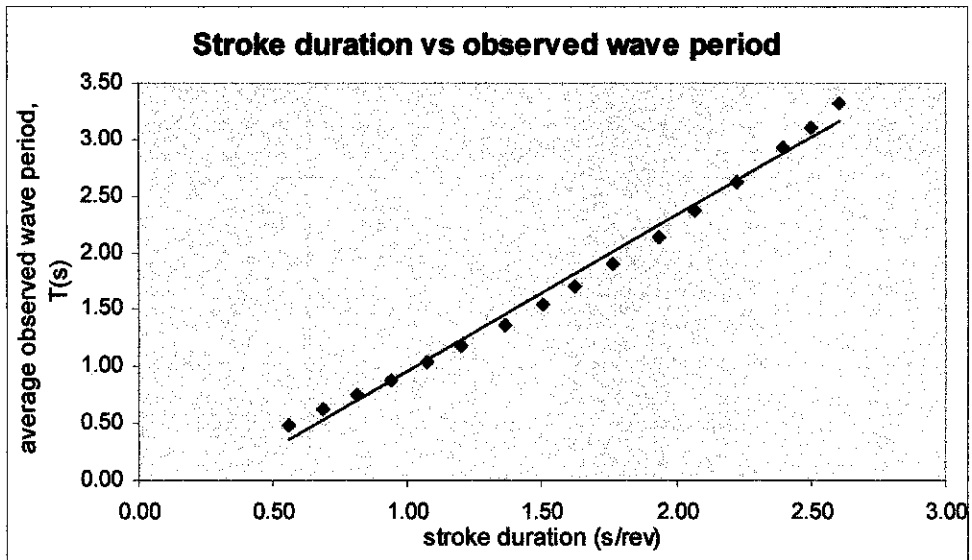


Figure 5.2: Stroke duration vs average observed wave period.

Figure 5.2 shows plot of average observed wave period with stroke duration. The graph shows the wave period increases linearly with increasing stroke duration. Suppose that the average wave period values is most likely the same with the stroke duration since the time taken for one completed cycle of wave period is equal to time for one complete revolution of the crank disc. The differences are contributed by human errors during recording time and mechanical error of the stroke system. The relationship between wave period and stroke duration is expressed in the equation

$$T = 1.3673S - 0.4095 \quad (5.2)$$

where T = observed wave period (s) and S = stroke duration (s/rev)

5.3 Determination of Incident Wave Height, H_i

Determination of incident wave height had been done in a series of sixteen wave period, ranging from 0.5 seconds to 3.3 seconds. The results are presented graphically in Figure 5.3. The experiments had been conducted in three water depths; 20 cm, 25 cm, and 30 cm with three different stroke adjustments; 80 mm, 140 mm, and 200 mm mainly to observe the characteristic of wave in various conditions.

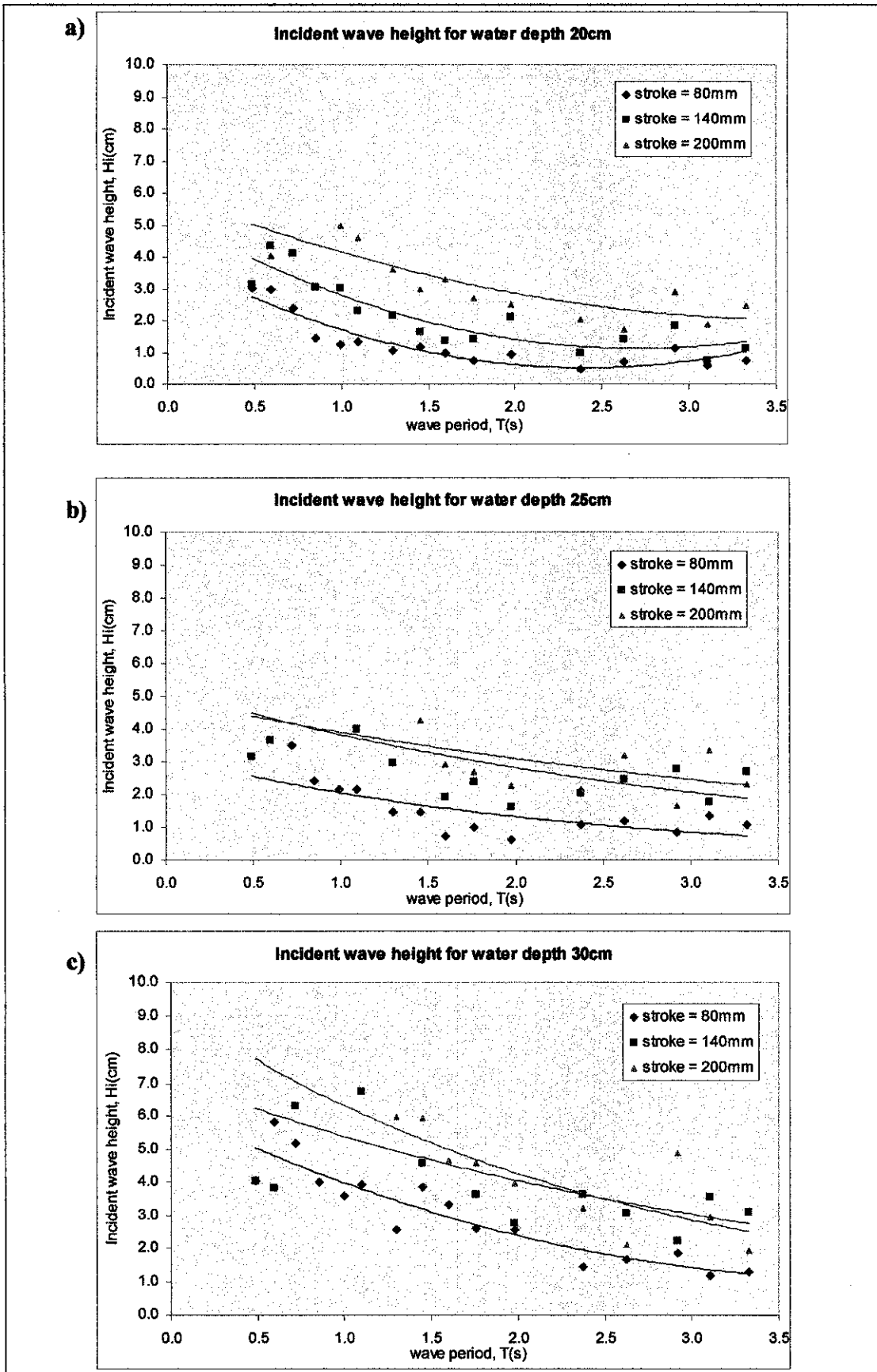


Figure 5.3: Incident wave height for three water depths; a) 20 cm, b) 25 cm, and c) 30 cm.

From Figure 5.3, it is observed that all curves are having the same trend, as the wave period increase, observed wave height decreases gradually. In each graph, 200 mm stroke adjustment give higher range wave heights than 140 mm and 80 mm stroke adjustment. It is also observed that wave height in 20 cm water depth have smaller range of wave height compared to wave height in 25 cm and 30 cm water depth as presented in Table 5.2.

Table 5.2: Incident wave height range for three water depths (20 cm, 25 cm, and 30 cm).

Water depth	Range of incident wave height (cm)			Overall range of incident wave height (cm)
	Stroke = 80mm	Stroke = 140mm	Stroke = 200mm	
20 cm	2.0 - 5.0	1.2 - 4.0	0.5 - 2.8	0.5 - 5.0
25 cm	2.2 - 4.4	1.8 - 4.5	0.8 - 2.5	0.8 - 4.5
30 cm	2.5 - 7.5	2.5 - 6.2	1.2 - 5.0	1.2 - 7.5

Referring to Table 5.2, overall range of incident wave heights increases as water depth and stroke adjustment increases. The variation of the values is mainly contributed by non-uniformity of waves formed by the wave generator. Another error is contributed by parallax errors during measurement process in determining of wave heights.

Table 5.2 also shows that the range of incident wave heights for particular water depth increases as the stroke adjustment increases especially in 30 cm water depth. Due to large range of incident wave heights for a particular stroke adjustment in a water depth, the next analysis will be based on H_i/gT^2 ; a dimensionless parameter to represent wave steepness in order to obtain better analysis from the experimental results.

From the analysis of the results, we can conclude that the incident wave height is dependent on water depth and wave period. The next step is to determine reflected wave height, H_r and transmitted wave height, H_t after installation of WSS and IWSS, and analyze the performance in terms of reflection coefficient, C_r and transmission coefficient, C_t .

5.4 Wave Suppress System (WSS)

The combination of all three water depths is illustrated in Figure 5.4. From the Figure 5.4 (a), the plots show that the range of C_r values is from 0.1 to 0.4. It is noted that the C_r values increase as H/gT^2 increases or water depth decreases.

Average C_r values for all water depths have been summarized in Table 5.3. From the table, again we can conclude that as water depth increases, the C_r value decreases. It is principally attributed to the ratio of breakwater draft-to-water depth D/d that controls the flow of water part beneath the floating structure. Apparently, 20 cm water depth will have the highest D/d ratio, which is 0.33 compared to 30 cm water depth, which is 0.22. In 20 cm water depth, almost 33% of the water column is obstructed by the floating structure present, thereby posing much wave energy been reflected back to the seaside. Thus the reflection effect in 20 cm water depth is more dominant than that in 30 cm water depth. However, the amount of energy reflected from WSS is considered small since maximum reflected wave height is 44%, which indicates that WSS is not a good reflector.

Figure 5.4 (b) shows the transmission coefficients for WSS. The figure shows same trend of curves for all three water depths, where C_t values decline gradually as H/gT^2 increases. The curves further show that C_t value increases with the increasing water depth. For example, at $H/gT^2 = 0.8$, C_t value is 0.45, 0.58 and 0.68 for water depth 20 cm, 25 cm and 30 cm respectively. This indicates that WSS applied in 20 cm water depth gives better wave attenuation performance than 25 cm and 30 cm water depth. This is because greater wave reflection effect found in 20 cm water depth compared to 25 cm and 30 cm water depth, thus fewer waves are transmitted to the leeside of WSS. From this, it is found that WSS is relatively effective in taking the wave energy out of the wave system when it is located at a site which is subjected to waves with high steepness (short period waves but great in height) and shallow water.

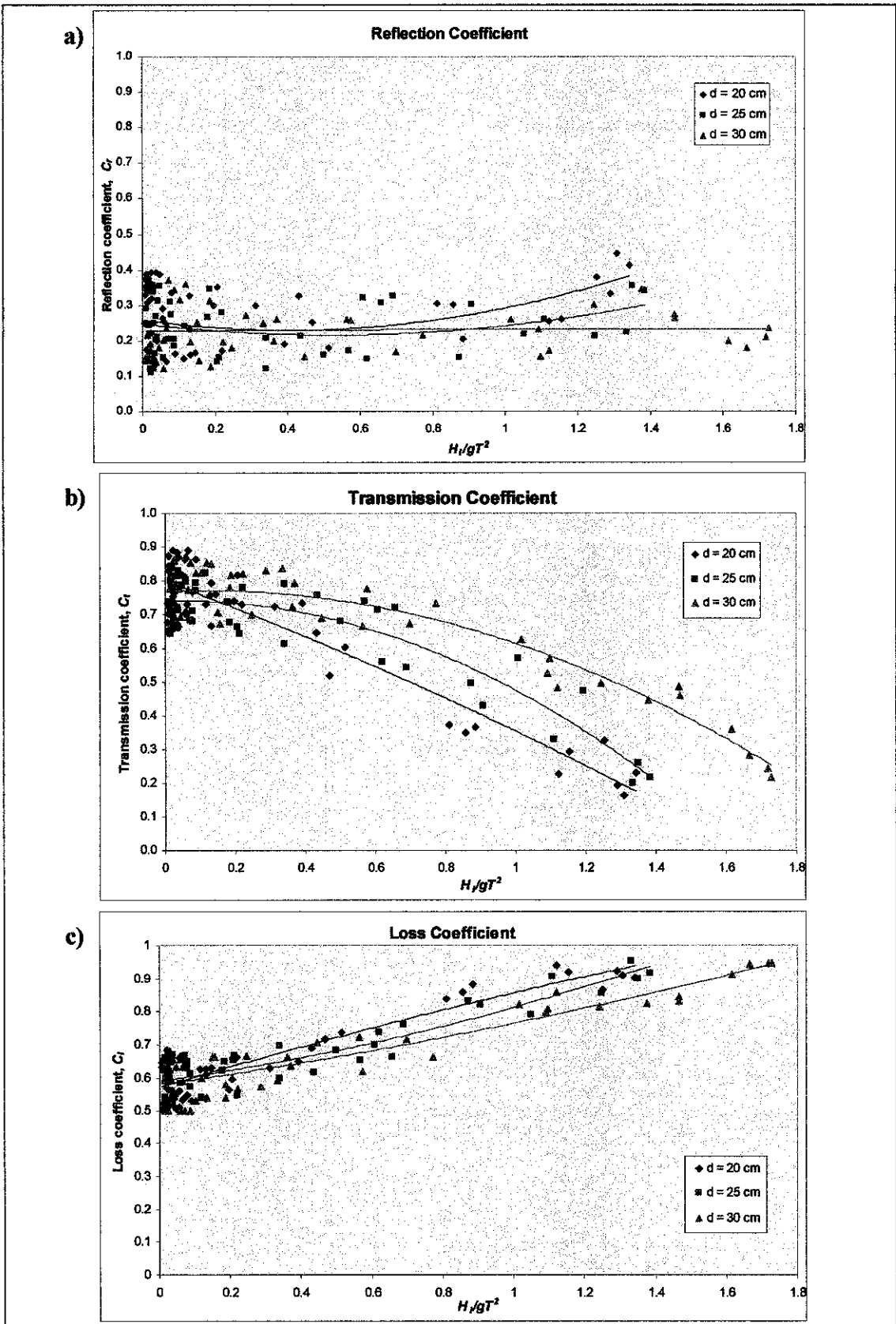


Figure 5.4: Reflection coefficient, Transmission coefficient, and Loss coefficient for WSS system.

Table 5.3: Average Reflection coefficient, C_r and D/d ratio for three water depths.

Water depth	Average reflection coefficient, C_r	D/d
20cm	0.25	$6.5/20 = 0.325$
25cm	0.24	$6.5/25 = 0.26$
30cm	0.22	$6.5/30 = 0.22$

where D = draft and d = water depth

Figure 5.4 (c) shows the loss coefficients for all three water depth. The figure shows increasing C_l with increasing H_l/gT^2 and with decreasing of water depth. Increasing value of loss coefficients indicates greater amount of energy is lost. As waves become steeper (increase value of H_l/gT^2), the wavelength is shorten and breaks on the structure, dissipating the wave energy to the system. Flatter waves however transmitted easily underneath or over the structure to the leeside; therefore, less energy is dissipated. Range of loss coefficients for various water depths is summarized in Table 5.4. From the table, the WSS is able to attenuate the wave energy at a minimum of 50% and a maximum of 95%. From previous discussion, the reflection coefficient analysis indicates that WSS is not a good reflector. However, it is indeed a good dissipator, as the C_l value achieved is as high as 0.95.

Table 5.4: Range of loss coefficient, C_l for three water depths.

Water depth	Range of loss coefficient, C_l
20 cm	0.50 – 0.94
25 cm	0.50 – 0.94
30 cm	0.50 – 0.95

5.5 Improved Wave Suppress System (IWSS)

Figure 5.5 (a) shows reflection coefficients for 3 water depths; 20 cm, 25 cm and 30 cm. From the figure, it can be observed that the curves have the same trend with WSS, where reflection coefficients increase as H_i/gT^2 increases. Increase in incident wave height, H_i and shorter wave period, T has enhance the wave reflection phenomena at the front of the model. It is also noted that as water depth increases, the reflection coefficients of IWSS model decrease.

The range of C_r for all water depths are summarized in Table 5.5. Water depth of 20 cm produce the highest range of reflection coefficients (up to 0.6 when $H_i/gT^2 = 1.31$), followed by those in 25 cm and 30 cm depth. This is because ratio of draft-to-water depth D/d obtained when $d = 20$ cm is high, causing great portion of water column is being obstructed by IWSS. Therefore, the incident waves are reflected to the seaside of the IWSS. The highest C_r values achieved as $d = 20$ cm is 0.58, indicates that the improved design of IWSS has enhance the reflection mechanism.

Table 5.5: Range of C_r values and D/d for three water depths.

Water depth	Range of C_r values	D/d
20cm	0.30 – 0.58	$5.0/20 = 0.25$
25cm	0.28 – 0.52	$5.0/25 = 0.20$
30cm	0.18 – 0.50	$5.0/30 = 0.17$

Figure 5.5 (b) shows the transmission coefficient of IWSS system. Similar to the transmission performance of WSS, C_t values decrease as H_i/gT^2 increases or water depth decreases. From the figure, it is noticed that at $0 < H_i/gT^2 < 0.2$, the values of C_t are closely to each other, which at $0.65 < C_t < 0.75$. This indicates that H_i/gT^2 is less dependent on water depth but highly dependent on wave period. The figure also shows that the graph representing 20 cm water depth produced the lowest C_t . This is because most of the waves at 20 cm water depth have been reflected to the seaside, thus fewer waves are transmitted to the leeside of IWSS. IWSS also capable of attenuating incident wave height up to 83% in 20 cm water depth.

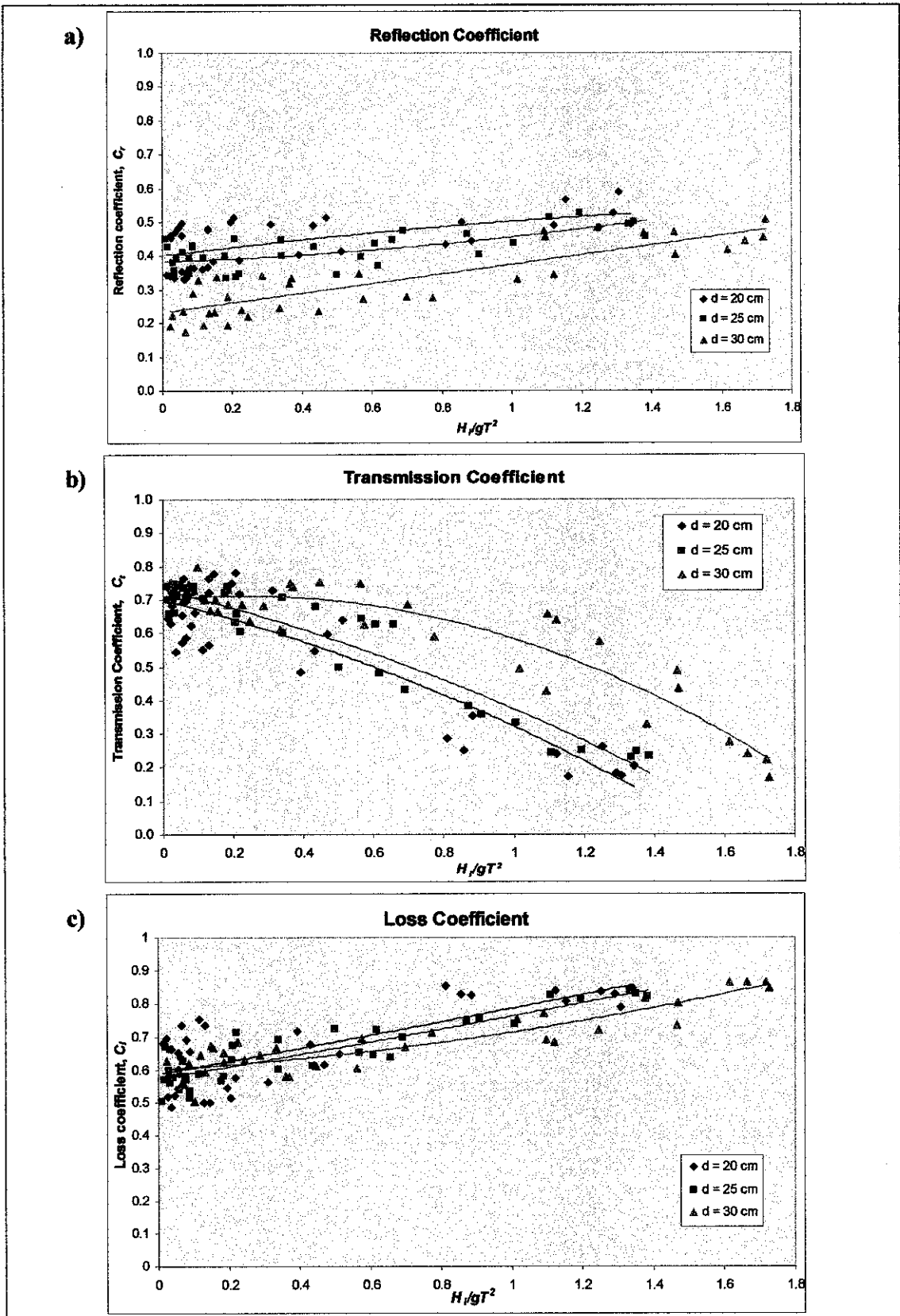


Figure 5.5: Reflection coefficient, Transmission coefficient, and Loss coefficient for IWSS system.

Figure 5.5 (c) shows the loss coefficient for IWSS system. From the figure, all the curves are ascending as H_i/gT^2 increases or as water depth decreases. It is observed that the graph representing 20 cm water depth produces the highest C_t , followed by that of 25 cm and 30 cm water depth. However the C_t curves are closely related with each other, which mean that IWSS is having similar degree of wave dissipation mechanism in all water depths. The figure also shows that IWSS is only capable to dissipate wave energy through wave breaking, friction and overtopping up to 86%, compared to 95% for WSS. This phenomenon occurred because much wave energy has been reduced by reflection action of IWSS, thus less energy is dissipated by the system and less energy is transmitted to the leeside as illustrated in Plate 5.1. From this, we can conclude that the significant mechanism of reducing wave energy of IWSS is reflection.

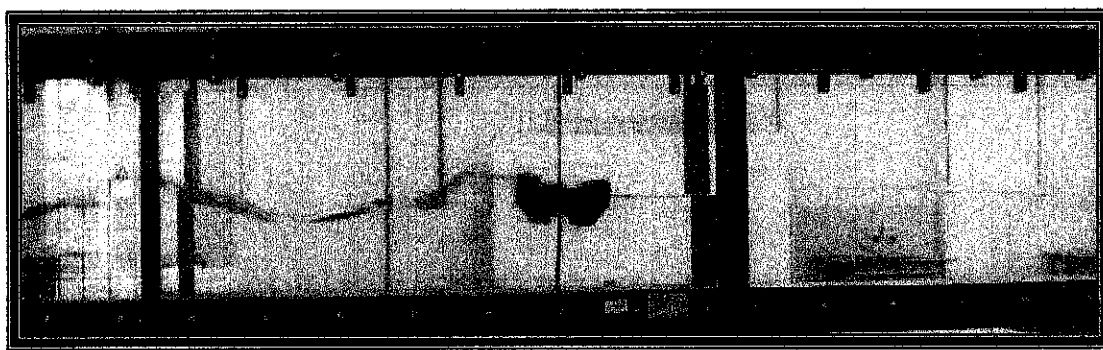


Plate 5.1: Wave dissipation mechanism of IWSS.

5.6 Improved Wave Suppress System with keel plate

The IWSS with addition of keel plate underneath the structure was studied thoroughly to investigate wave attenuation capacity of this special feature. The experimental results are presented in Figure 5.6, which shows the variation of C_t , C_r , and C_l with H_i/gT^2 ranging from 0.0 to 1.8.

Figure 5.6 (a) shows C_r increases with the increase of H_i/gT^2 . It is further observed that as the water depth increase, the C_r values also increases. The figure also shows that the highest wave reflection occurs when $d = 20$ cm. Table 5.6 shows that the addition of keel plate to the IWSS has increase the draft of the breakwater system and produce higher D/d ratio. With the enhanced of D/d ratio, the breakwater become a better barrier obstructing the incoming flow of water. Therefore, higher waves reflection will be

expected as illustrated in Plate 5.2. The results also support that C_r is directly proportional to D/d ratio. This also confirms that draft is one of the key factors that will affect the performance of floating breakwaters.

Table 5.6: Range of C_r values and D/d for three water depths.

Water depth	Range of C_r values	D/d
20cm	0.38 – 0.81	$10.3/20 = 0.52$
25cm	0.27 – 0.70	$10.3/25 = 0.41$
30cm	0.20 – 0.61	$10.3/30 = 0.34$



Plate 5.2: Higher wave reflection for IWSS with keel plate.

Figure 5.6 (b) shows variation of transmission coefficients for three water depths. Similar with the previous transmission coefficient analysis, C_t reduced gradually with an increase of H/gT^2 . C_t also increases as water depth increase. Again, C_t of $d = 20$ cm gave the best wave attenuation performance, which is 0.12 at $H/gT^2 = 1.25$. H/gT^2 , which is wave steepness is a strong parameter that affect C_t values. The steeper the wave, where incident wave is higher or shorter wave period, the better will be the attenuation of the wave energy.

Figure 5.6 (c) shows that loss coefficient for the system increase gradually with the increasing of H/gT^2 . C_l values also decrease as water depth increases but the difference is not very significant. At $H/gT^2 = 0.2$, the C_l values are the same which is 0.58. As expected, 20 cm water depth produce highest C_l , which is 0.77 at $H/gT^2 = 1.34$. From C_r and C_t analysis, this system shows that the breakwater is not a good dissipator, but it is a reflector type breakwater.

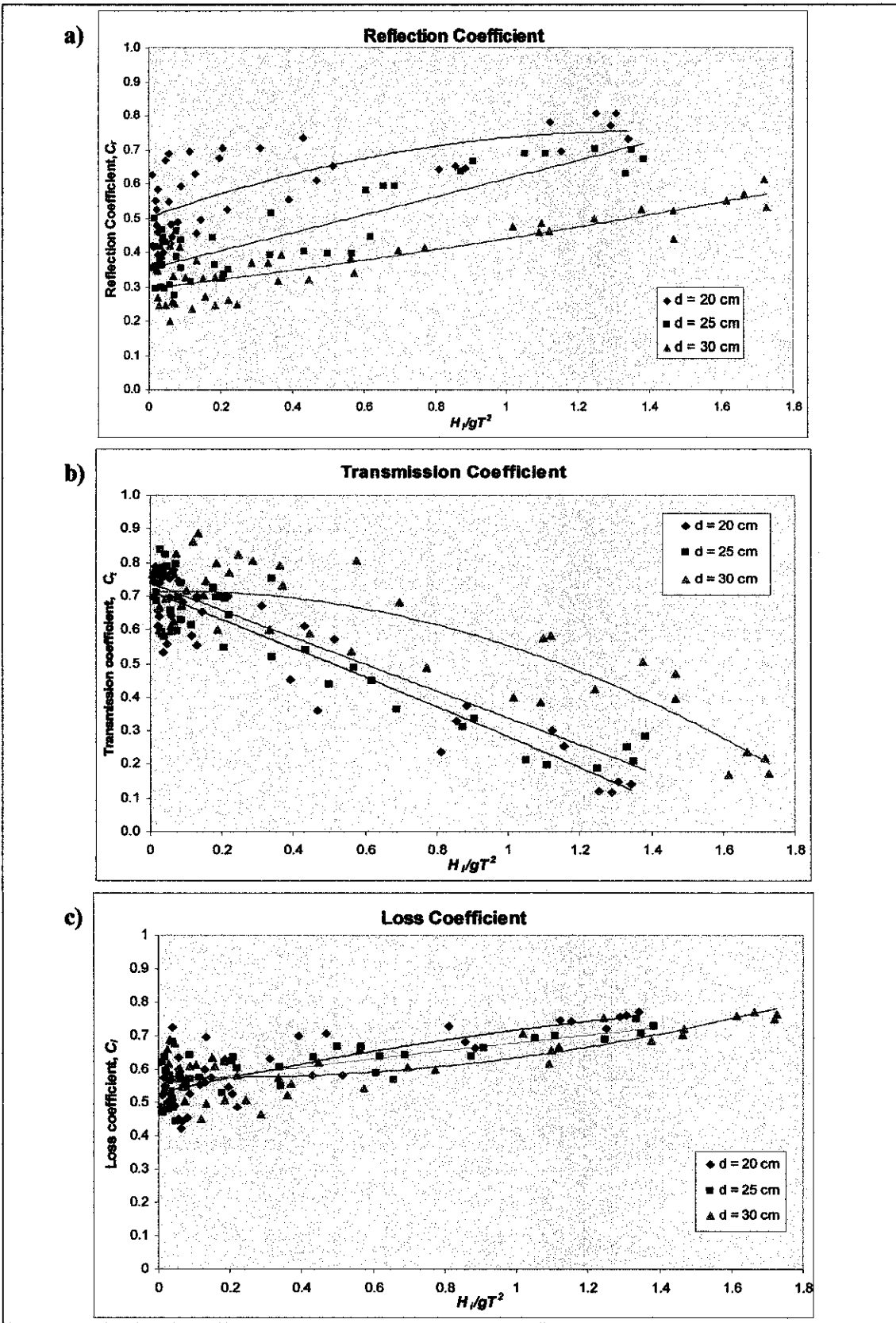


Figure 5.6: Reflection coefficient, Transmission coefficient, and Loss coefficient for IWSS with keel plate system.

5.7 Comparison of WSS and IWSS performances

In order to know whether IWSS system has improved from WSS system, a comparison of each system has been made according to different water depths. Figure 5.7 shows comparison of reflection coefficients for three systems, which are WSS, IWSS and IWSS with keel plate in water depth of 20 cm, 25 cm and 30 cm.

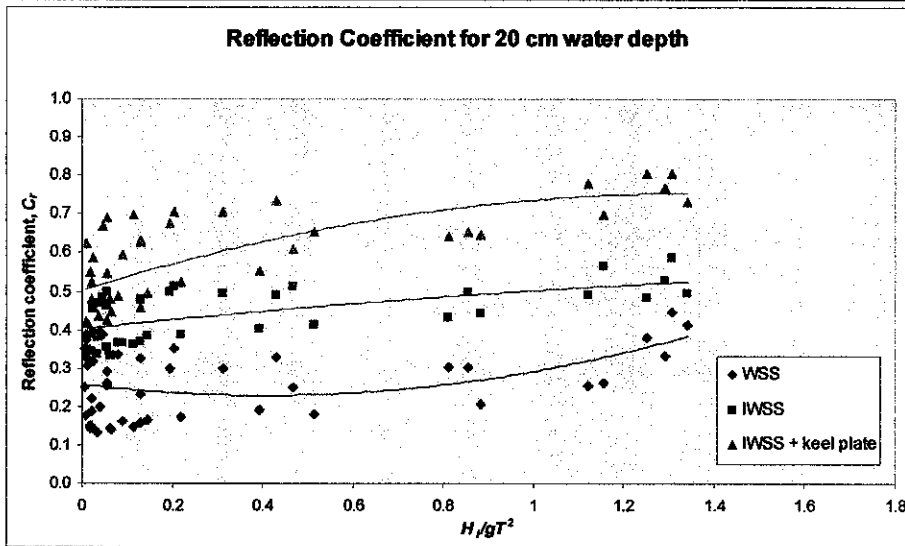
From Figure 5.7, it is noted that C_r values increase as H/gT^2 increases for all water depths. We also can see that IWSS with keel has the highest C_r values when $0 < H/gT^2 < 1.4$ for all water depths, followed by IWSS and WSS. This obviously verifies that IWSS system has improved the wave reflection ability especially with attachment of keel plate from the main structure. Table 5.7 shows the range of C_r values and D/d ratio for each model in three water depths.

Table 5.7: Range of reflection coefficients and D/d ratio.

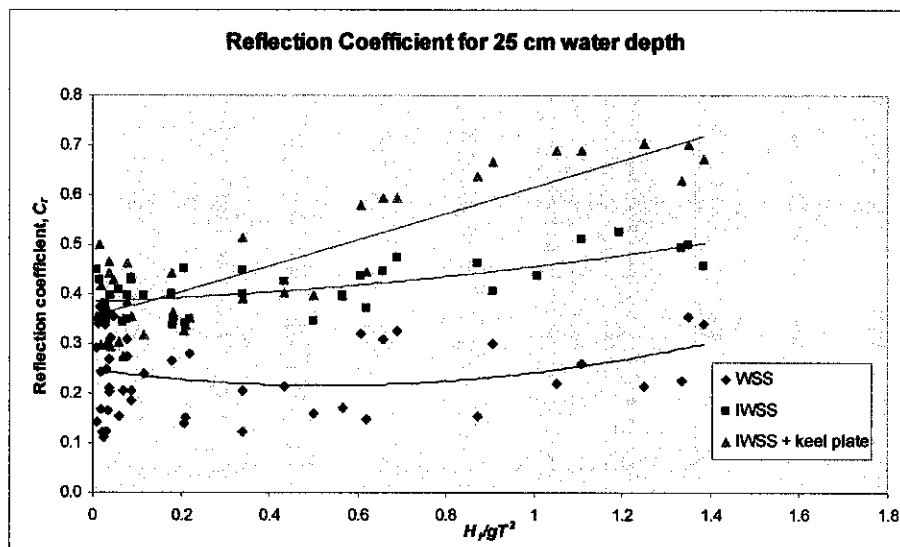
Water depth	Model	Range of C_r values	D/d ratio
20 cm	WSS	0.14 – 0.45	0.33
	IWSS	0.30 – 0.58	0.25
	IWSS + keel plate	0.38 – 0.81	0.52
25 cm	WSS	0.11 – 0.37	0.26
	IWSS	0.28 – 0.52	0.20
	IWSS + keel plate	0.27 – 0.70	0.41
30 cm	WSS	0.12 – 0.37	0.22
	IWSS	0.18 – 0.50	0.17
	IWSS + keel plate	0.20 – 0.61	0.34

From the table, 20 cm water depth produce the highest C_r range compared to 25 cm and 30 cm water depth. As explained before, it is due to high D/d ratio compared to those of other water depths, in which most of the water column is obstructed by the structure. IWSS with keel model acts as a vertical barrier, preventing waves to transmit underneath the structure. Even though IWSS model has lower D/d ratio compared to WSS, the C_r values are still higher. This is because of the slanting feature of the bottom structure directly reflects the wave energy to the seaward side of the structure.

a)



b)



c)

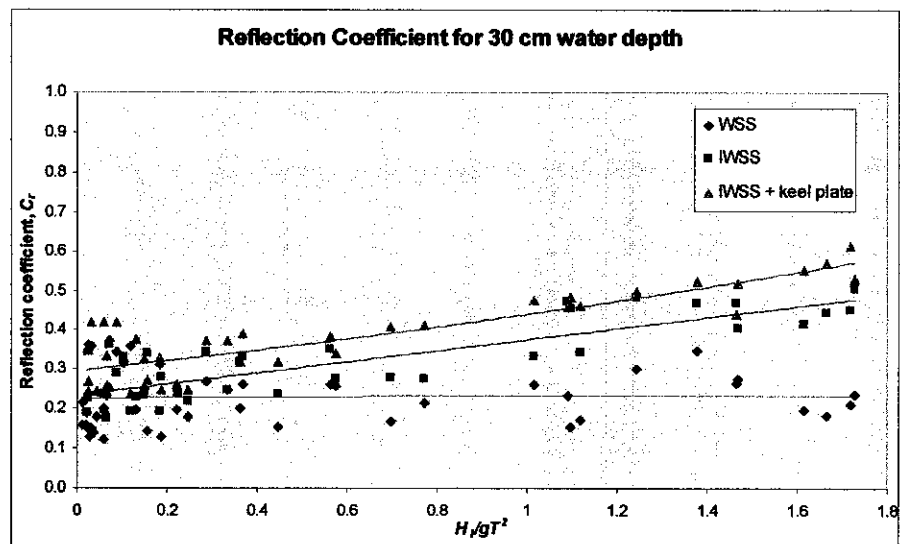


Figure 5.7: Reflection coefficients for a) 20 cm, b) 25 cm, and c) 30 cm water depth.

From the above analysis, we can conclude that IWSS with keel plate is the best reflector, followed by IWSS model, which each capable to reflect maximum of 81% and 58% of waves to the seaside. WSS model is not a good reflector since only average of 25% of waves is reflected to the seaside.

Comparison of transmission coefficients between three models has been presented in Figure 5.8. The plots representing different floating breakwaters show a similar trend, which C_t values decrease as H_s/gT^2 increases, for water depth of 20 cm, 25 cm and 30 cm. The figure shows that IWSS with keel plate produced lowest C_t values, followed by IWSS, and WSS. Table 5.8 summarize the range of C_t for each model in three water depths.

From the table, all models produced lowest C_t values in 20 cm water depth. This is due to most of the wave energy is reflected to the seaside. As for the conclusion, IWSS with keel plate model has improved tremendously in attenuating wave energy up to 88% in short wave period waves.

Table 5.8: Range of transmission coefficients.

Water depth	Model	Range of C_t values
20 cm	WSS	0.16 – 0.89
	IWSS	0.17 – 0.78
	IWSS + keel plate	0.12 – 0.78
25 cm	WSS	0.20 – 0.84
	IWSS	0.23 – 0.75
	IWSS + keel plate	0.19 – 0.84
30 cm	WSS	0.22 – 0.86
	IWSS	0.17 – 0.80
	IWSS + keel plate	0.17 – 0.89

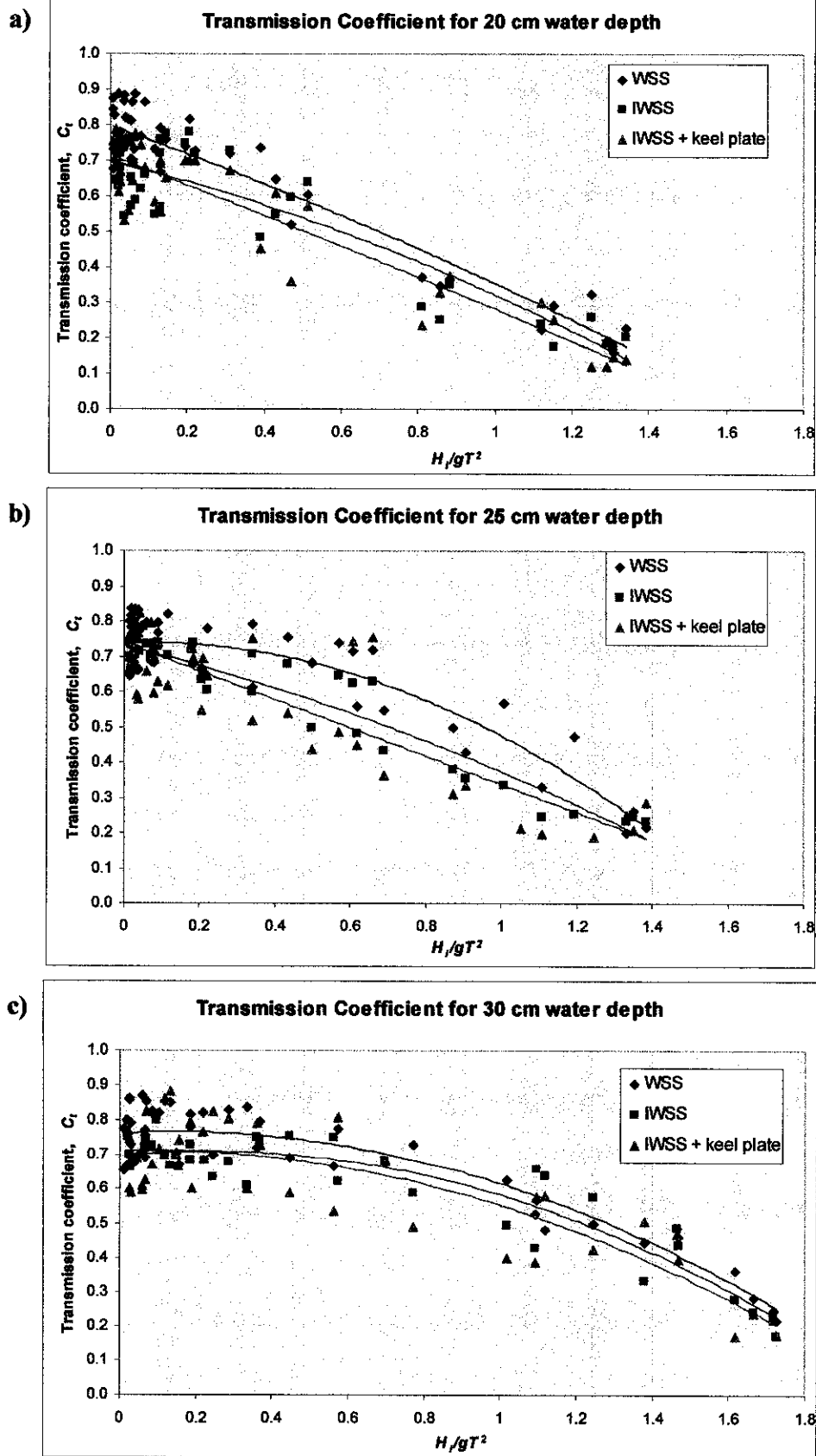


Figure 5.8: Transmission coefficients for a) 20 cm, b) 25 cm, and c) 30 cm water depth.

Calculation of loss coefficient for all models has been made using Equation 2.7 and the graphs are presented in Figure 5.9. The figure shows that C_t values increase as H_i/gT^2 increases for all water depths. The curves also lie in a similar trend, which high C_t values occurred when the structure is exposed to steep waves. The wave energy dissipates through breaking, overtopping and friction on the structure. It is also noted that WSS have highest C_t values in all three water depths, followed by IWSS and IWSS with keel plate. This indicates that WSS is a better dissipator, even though it is not a good reflector. Summary of range of loss coefficients has been tabulated in Table 5.9.

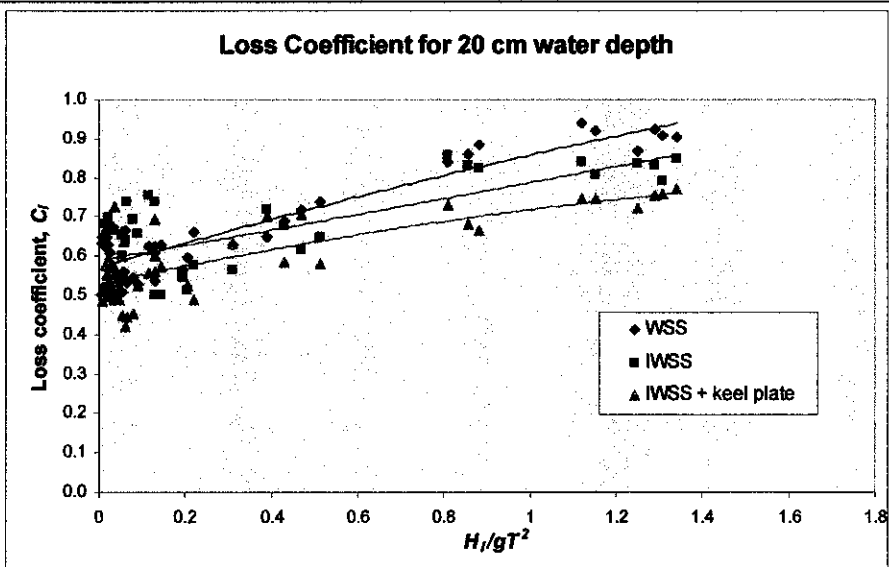
Referring the Table 5.9, all models are capable of dissipating minimum of 40% wave energy by the system. WSS, IWSS and IWSS with keel plate is capable of dissipating wave energy up to 95%, 87% and 77% respectively. IWSS with keel plate has lowest C_t and highest C_r , which means that the model use reflection as the main mechanism to reduce the wave energy. Thus only small portion of waves is dissipated by the structure, which means that the model is not a good dissipator.

For the conclusion, comparison of all models according to water depth has shown that all models performed very well in 20 cm water depth. The analysis also has indicated that IWSS with keel plate model is a good reflector and WSS model is a good dissipator. All in all, improvement on performance of WSS is successful and has met the objectives.

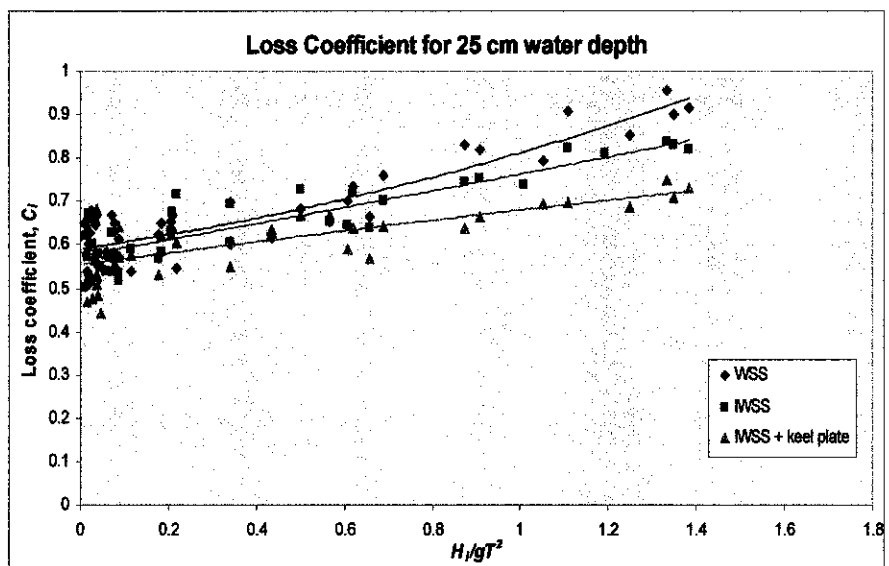
Table 5.9: Range of loss coefficients.

Water depth	Model	Range of C_t values
20 cm	WSS	0.50 – 0.94
	IWSS	0.49 – 0.85
	IWSS + keel plate	0.48 – 0.76
25 cm	WSS	0.50 – 0.94
	IWSS	0.50 – 0.84
	IWSS + keel plate	0.44 – 0.75
30 cm	WSS	0.50 – 0.95
	IWSS	0.50 – 0.87
	IWSS + keel plate	0.45 – 0.77

a)



b)



c)

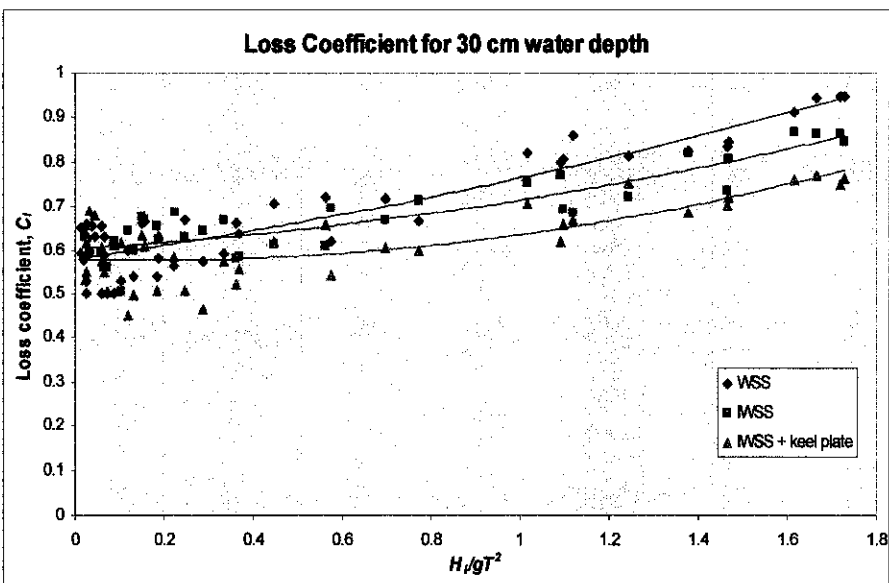


Figure 5.9: Loss coefficients for a) 20 cm, b) 25 cm, and c) 30 cm water depth.

5.8 Determination of Wavelength, L .

The length of waves generated from wave facility was calculated with the reference from Table C-1 Shore Protection Manual (US Army, 1983). The steps of obtaining wavelength with respect to wave period and water depth are explained as follows:

1. Calculate deep water wavelength, L_o for each wave period. ($L_o = gT^2 / 2\pi$).
2. Calculate d/L_o for each water depth.
3. Refer to Table C-1 Shore Protection Manual to obtain d/L value.
4. Classify the wave to deep water, transitional water or shallow water, based on the following requirements:
 - $d/L \geq 0.5 \rightarrow$ deep water.
 - $0.04 \leq d/L \leq 0.5 \rightarrow$ transitional water.
 - $d/L \leq 0.04 \rightarrow$ shallow water.
5. Determine wavelength.

The calculation of wavelength is tabulated in Table 5.10, 5.11 and 5.12. Figure 5.10 shows plot of relative depth, d/L for wave period ranging from 0.5 to 3.3 seconds in water depth of 20 cm, 25 cm, and 30 cm respectively.

Table 5.10: Determination of wavelength, L for 20 cm water depth.

Observed wave period, T (s)	Deep water wavelength, L_o (m)	d/L_o	d/L	Wavelength, L (m)
0.49	0.37	0.5376	0.53890	0.37
0.60	0.55	0.3611	0.36830	0.54
0.72	0.81	0.2475	0.26570	0.75
0.85	1.13	0.1769	0.20570	0.97
0.99	1.54	0.1297	0.16640	1.20
1.09	1.87	0.1072	0.14720	1.36
1.30	2.63	0.0761	0.11960	1.67
1.45	3.29	0.0609	0.10520	1.90
1.60	3.98	0.0503	0.09447	2.12
1.76	4.83	0.0414	0.08486	2.36
1.98	6.10	0.0328	0.07483	2.67
2.37	8.79	0.0228	0.06171	3.24
2.63	10.75	0.0186	0.05549	3.60
2.92	13.32	0.0150	0.04964	4.03
3.11	15.05	0.0133	0.04666	4.29
3.32	17.24	0.0116	0.04349	4.60

Table 5.11: Determination of wavelength, L for 25 cm water depth.

Observed wave period, T (s)	Deep water wavelength, L_o (m)	d/L_o	d/L	Wavelength, L (m)
0.49	0.37	0.6720	0.6723	0.37
0.60	0.55	0.4513	0.4543	0.55
0.72	0.81	0.3094	0.3206	0.78
0.85	1.13	0.2212	0.2431	1.03
0.99	1.54	0.1621	0.1934	1.29
1.09	1.87	0.1340	0.1699	1.47
1.30	2.63	0.0951	0.1367	1.83
1.45	3.29	0.0761	0.1196	2.09
1.60	3.98	0.0629	0.1072	2.33
1.76	4.83	0.0518	0.09602	2.60
1.98	6.10	0.0410	0.08442	2.96
2.37	8.79	0.0284	0.0693	3.61
2.63	10.75	0.0233	0.06242	4.01
2.92	13.32	0.0188	0.05578	4.48
3.11	15.05	0.0166	0.0523	4.78
3.32	17.24	0.0145	0.04878	5.13

Table 5.12: Determination of wavelength, L for 30 cm water depth.

Observed wave period, T (s)	Deep water wavelength, L_0 (m)	d/L_0	d/L	Wavelength, L (m)
0.49	0.37	0.8064	0.80650	0.37
0.60	0.55	0.5416	0.54280	0.55
0.72	0.81	0.3713	0.37780	0.79
0.85	1.13	0.2654	0.28140	1.07
0.99	1.54	0.1945	0.22050	1.36
1.09	1.87	0.1607	0.19230	1.56
1.30	2.63	0.1141	0.15310	1.96
1.45	3.29	0.0913	0.13340	2.25
1.60	3.98	0.0755	0.11910	2.52
1.76	4.83	0.0621	0.10640	2.82
1.98	6.10	0.0492	0.09332	3.21
2.37	8.79	0.0341	0.07642	3.93
2.63	10.75	0.0279	0.06865	4.37
2.92	13.32	0.0225	0.06129	4.89
3.11	15.05	0.0199	0.05748	5.22
3.32	17.24	0.0174	0.05350	5.61

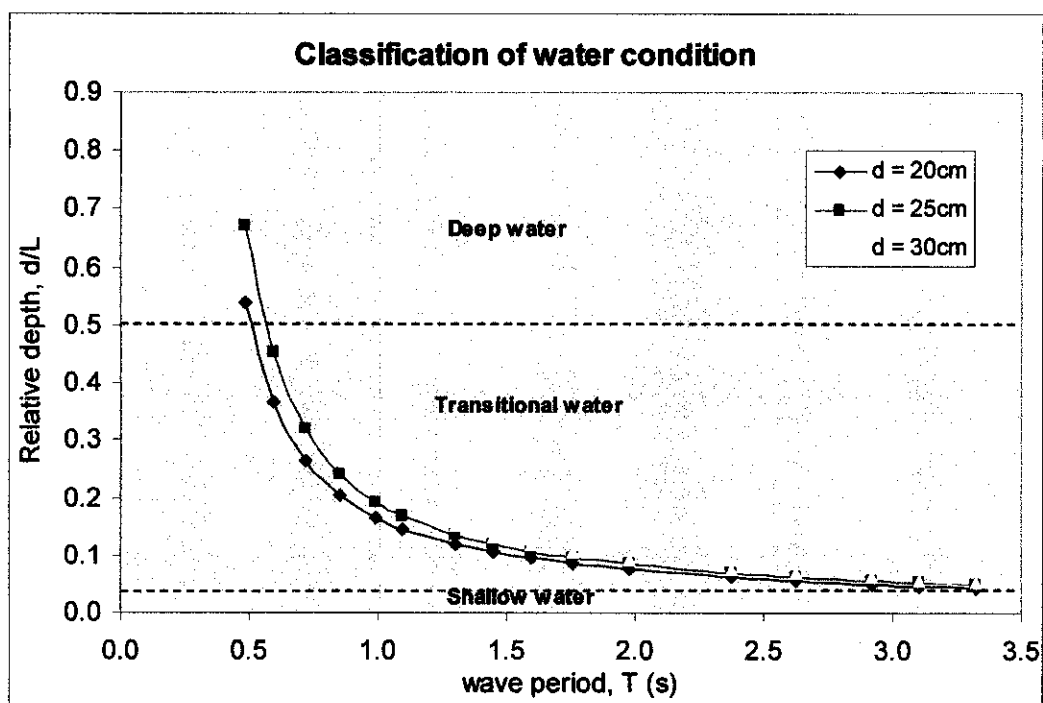


Figure 5.10: Classification of water condition.

From Figure 5.10, waves with period less than 0.5 seconds are deep water waves, waves with period from 0.5 seconds to 3.3 seconds are transitional water wave, and waves with period more than 3.3 seconds are shallow water waves. As the wave period increases, d/L values decrease exponentially. Therefore, we can conclude that the experimental studies of the performance of WSS vary from deep water to transitional water conditions.

5.9 Comparison of Performance of IWSS with Previous Studies

The performance of previous studies of floating breakwaters in term of transmission coefficient and relative width ratio is illustrated in Figure 5.11. Relative width ratio is the ratio of width of the structure-to-wavelength. From the figure, all of the curves show similar trend and shape. The curves also show that the C_t value decreases as W/L increases in value. The graph indicates that the curves are laid at a range of W/L from 0.1 to 1.1.

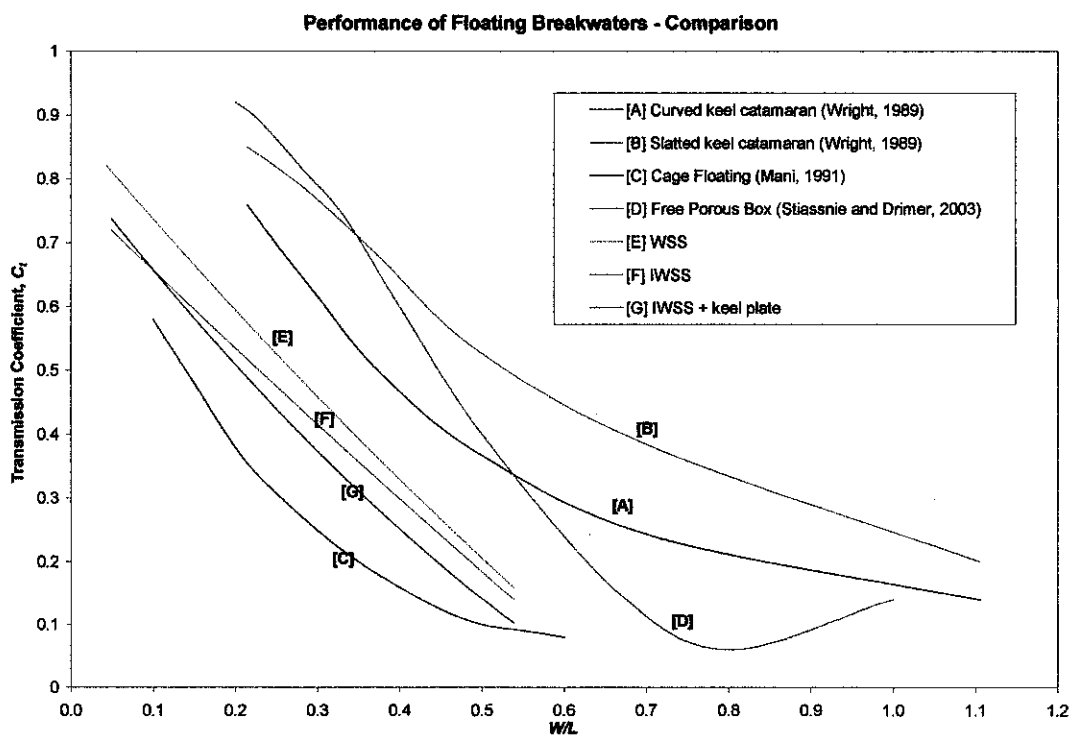


Figure 5.11: Comparison of Transmission Coefficient results with previous studies.

Curve [E], [F], and [G] is the experimental results of WSS, IWSS and IWSS with keel plate, respectively in 20 cm water depth. From the figure, it is obviously shown that IWSS models have improved the attenuation performance compared to WSS model. IWSS

with keel plate model has improved maximum of 10% relative to WSS model. From the graph, the experimental studies of WSS and IWSS were subjected to a range of 0.54 W/L due to the limitation of availability of the wave facility.

When we compare the performance of all floating breakwaters, Cage Floating Breakwater [C] and Free Porous Box [D] shows the best performance compared to others by attenuating wave energy more than 90%. Table 5.13 summarized the D/d ratio and W/d ratio for all models. From Table 5.13, model [A] and [B] has low D/d ratio, which is the main reasons that their performances are not as good as other models. It is also noticed that Free Porous Box has greater width compared to others which lead to low C_t values. Cage Floating Breakwater in other hand has lower D/d ratio compared to IWSS with keel plate but still managed to produce lower C_t values. This may contribute by other factors such as mooring line and wave dissipation mechanisms of the model itself. From the comparison analysis, it can be concluded that draft and width of the structure is the crucial features for development of floating breakwater.

Table 5.13: D/d ratio and W/d ratio

Model	D/d ratio	W/d ratio
[A] Curved keel catamaran	0.27	1.15
[B] Slatted keel catamaran	0.27	1.15
[C] Cage Floating Breakwater	0.46	0.8
[D] Free Porous Box	-	5
[E] WSS	0.33	1
[F] IWSS	0.25	1
[G] IWSS with keel plate	0.52	1

CHAPTER 6

CONCLUSION AND RECOMMENDATION

6.1 Conclusion

The development of IWSS has been studied and the performance shows that IWSS has improved the wave attenuation performance compared to WSS. Below are few conclusions that have been obtained from this project.

- Calibration of wave period in three different stroke adjustments has resulted the same wave period for all three stroke adjustments. This indicates that wave period does not depend on stroke adjustment but only depends on the stroke frequency which can be interpreted by equation

$$T = 152.52 f^{-1.2362}$$

where T = wave period (s) and f = stroke frequency (rpm)

- Determination of incident wave height, H_i indicates that as the wave period increases, the H_i decreases. H_i also increases as water depth increases. This shows that the incident wave height is dependent on wave period and water depth.
- Reflection coefficient analysis indicates that all IWSS models have improved the reflection mechanism as they reflect more waves than WSS model. The factor that contributed to the improvement is the slanting feature of IWSS and the increase of draft using keel plate. The best reflector is IWSS with solid keel plate followed by IWSS model itself and WSS model.

- Transmission coefficient analysis indicates that IWSS with keel plate can attenuate up to 88% of wave energy in 20 cm water depth which is at wave period less than 1 second. It is also found that all models are relatively effective with respect to high steepness waves (short period but great height) and shallow water.
- Loss coefficient analysis indicates that the WSS is a good dissipator compared to IWSS models, which is able to attenuate the wave energy up to 96%.
- Determination of wavelength indicates that experiments were conducted in transitional to deep water condition in the wave flume.
- Comparison with previous studies shows that IWSS models have improved the attenuation performance compared WSS model, which has met the objectives of the studies. It is also believed that draft and width of the structure is the crucial features for development of floating breakwater.

6.2 Recommendation

For improvement on the study of WSS performance, few recommendations are highlighted below.

- The improvement of design is concentrated on the effect of higher draft and porosity. The effect of width has not been studied due to time constraint. For further studies, it is recommended to analyze the performance of all models that is arranged in a number of rows. It has been verified by other researchers that increase in draft and width has a positive effect to the attenuation performance of floating breakwaters. Further studies also should consider analyzing the IWSS performance + keel with various openings.
- Experimental studies also could be improved by adding more friction to the structure in order to have higher loss due to the structure itself.
- The experimental studies also should be conducted in wide range of wave period, which is beyond 3 seconds in order to evaluate the performance of the models in long wave period.
- Further studies on the material of IWSS structure are essential for the improvement of water absorption characteristic which is a problem to the models. The studies will also provide alternative materials that can be used for the structure if IWSS is to be commercialized.
- Cost comparison between IWSS and other types of floating breakwaters should be considered to know whether IWSS is a cost effective structure or not since it can be fabricated locally compared to others.

REFERENCES

1. **Cox, R. J., Blumberg, G. P., and Wright, M. J.** September 1991. "Floating Breakwaters – Practical Performance Data", COPEDEC III – Third International Conference on Coastal and Port Engineering in Developing Countries Mombassa, Kenya.
2. **Murali, K., and Mani, J. S.** "Performance of Cage Floating Breakwater", Journal of Waterway, Port, Coastal, and Ocean Engineering, Vol. 123, No. 4, July/August, 1997.
3. **Drimer, N., and Stiassnie, M.** "On Freely Floating Porous Box in Shallow Water Waves", Applied Ocean Research 25 (2003) 263-268.
4. **Teh, H. M. and Ismail, H.** "Wave Attenuation Characteristics of a Stepped-Slope Floating Breakwater (SSFBW) System", Proceeding of 13th IAHR-APD Congress Singapore, 6th - 8th August 2002.
5. **Young, D. F., Munson, B. R., and Okiishi, T.H.** "A Brief Introduction to Fluid Mechanics, 2nd Edition, John Wiley & Sons, Inc. 2001.
6. **Gourlay, M. R., and Apelt, C.J.** "Coastal Hydraulics and Sediment Transport in a Coastal System", Department of Civil Engineering of the University of Queensland. 1983, pp 89-90.
7. **Sorenson, R. M.** "Basic Coastal Engineering", 2nd Edition, International Thompson Publishing, 1997, pp 202-205.
8. **Sorenson, R. M.** "Basic Wave Mechanics for Coastal and Ocean Engineers", John Wiley & Sons, Inc. 1993.
9. Table C-1 Shore Protection Manual (US Army, 1983).

10. **Noor Hidayah bt. Abdul Halim.** 2004. "Wave Energy Absorption Performance of Wave Absorbers", Universiti Teknologi PETRONAS.
11. **Wong Siew Lee.** December 2004. "Wave Damping Characteristics of Near Surface Submerged Breakwater System", Universiti Teknologi PETRONAS.

APPENDICES

Wave Absorber

Materials: floor mat, wood, wire mesh, rod, clamp, heavy materials to hold the absorber at the bottom (rock or brick).

Dimension: 120 cm (length) x 120 cm (slope) x 30cm (width) x 30-90cm (height).

Slope: min: 15°, max: 45°.

Calculation:

1. Lean (1967) recommended the absorber length should be at least 75% of incident wavelength to achieve reflection coefficient below 10%.
2. Ouellet and Datta (1986) concluded that wire mesh absorbers are more efficient for slope angles greater than 15 degrees.

	Water depth = 20cm		Water depth = 30cm	
	T = 0.5s	T = 1.5s	T = 0.5s	T = 1.5s
d/L	0.5144	0.1013	0.7693	0.1281
L	0.389m	1.97m	0.39m	2.34m

75% of 1.97m wavelength = 1.48m. Due to size limitation, design absorber length: 1.2m

For height of absorber, minimum height design is 30cm.

For minimum slope of 15°, length of the absorber is 112cm and length of slope is 116cm. So, 120cm design length is adequate.

For maximum slope of 45° with length of absorber 120cm, the height is 85cm. So the design height varies from 30cm to 90cm.

Calculation of IWSS

$$\begin{aligned} \text{Volume of breakwater, } V_B &= [(20 \times 10) - (3 \times 12 + 2 \times 6 + 4 \times 5)] \times 30 \times 10^{-6} \text{ m}^3 \\ &\quad + 24 \times 10^{-6} \text{ m}^3 \text{ (volume of porous plate)} \\ &= 3.984 \times 10^{-3} \text{ m}^3 \end{aligned}$$

$$\text{Targeted draft} = 5.5 \text{ cm}$$

$$\begin{aligned} \text{Volume submerged, } V_s &= [(20 \times 5.5) - (20 + 12)] \times 30 \times 10^{-6} + 24 \times 10^{-6} \text{ m}^3 \\ &= 2.364 \times 10^{-3} \text{ m}^3 \end{aligned}$$

$$\begin{aligned} \text{Buoyancy force, } F_B &= \gamma V_s \\ &= 9.8 \times 10^3 \times 2.364 \times 10^{-3} \\ &= 23.17 \text{ N} \end{aligned}$$

$$\begin{aligned} \text{Mass, } m_B &= F_B / g \\ &= 23.17 / 9.81 \\ &= 2.36 \text{ kg} \end{aligned}$$

$$\begin{aligned} \text{Density, } \rho_B &= 2.36 \text{ kg} / 3.984 \times 10^{-3} \text{ m}^3 \\ &= 592.77 \text{ kg/m}^3 \end{aligned}$$

Density of ALC = 500 kg/m^3 and density of zinc sheet = 7870 kg/m^3 ;

$$\begin{aligned} \text{Weight of breakwater, } W_B &= [500 \text{ kg/m}^3 (3.96 \times 10^{-3} \text{ m}^3) + 7870 \text{ kg/m}^3 (24 \times 10^{-6} \text{ m}^3)] \\ &\quad \times 9.81 \text{ N/kg} \\ &= 21.3 \text{ N} \end{aligned}$$

Since F_B is greater than W_B , the breakwater will float.

Determination of draft and freeboard

For IWSS without porous plate:

$$\text{Volume of breakwater, } V_B = 3.96 \times 10^{-3} \text{ m}^3$$

$$\begin{aligned} \text{Volume submerged, } V_s &= [(20 \times \text{draft}) - (20 + 12)] \times 30 \times 10^{-6} \text{ m}^3 \\ &= 6 \times 10^{-4} \times \text{draft} - 9.6 \times 10^{-4} \text{ m}^3 \end{aligned}$$

$$\begin{aligned} \text{Buoyancy force, } F_B &= \gamma V_s \\ &= 9.8 \times 10^3 (6 \times 10^{-4} \times \text{draft} - 9.6 \times 10^{-4} \text{ m}^3) \\ &= 5.88 \times \text{draft} - 9.408 \text{ N} \end{aligned}$$

$$\begin{aligned} \text{Weight of breakwater, } W_B &= 500 \text{ kg/m}^3 \times 3.96 \times 10^{-3} \text{ m}^3 \times 9.81 \text{ N/kg} \\ &= 19.42 \text{ N} \end{aligned}$$

$$\begin{aligned} \text{Weight of breakwater, } W_B &= \text{Buoyancy force, } F_B \\ 19.42 \text{ N} &= 5.88 \times \text{draft} - 9.408 \text{ N} \end{aligned}$$

$$\begin{aligned} \text{Draft} &= 4.9 \text{ cm} \\ \text{Freeboard} &= 5.1 \text{ cm} \end{aligned}$$

For IWSS with porous plate;

$$\text{Volume of breakwater, } V_B = 3.984 \times 10^{-3} \text{ m}^3$$

$$\begin{aligned} \text{Volume submerged, } V_S &= [(20 \times \text{draft}) - (20 + 12)]30 \times 10^{-6} + 24 \times 10^{-6} \text{ m}^3 \\ &= 6 \times 10^{-4} \times \text{draft} - 9.36 \times 10^{-4} \text{ m}^3 \end{aligned}$$

$$\begin{aligned} \text{Buoyancy force, } F_B &= \gamma V_S \\ &= 9.8 \times 10^3 (6 \times 10^{-4} \times \text{draft} - 9.6 \times 10^{-4} \text{ m}^3) \\ &= 5.88 \times \text{draft} - 9.173 \text{ N} \end{aligned}$$

$$\text{Weight of breakwater, } W_B = 21.3 \text{ N}$$

$$\begin{aligned} \text{Weight of breakwater, } W_B &= \text{Buoyancy force, } F_B \\ 21.3 \text{ N} &= 5.88 \times \text{draft} - 9.173 \text{ N} \\ \text{draft} &= 5.18 \text{ cm, plus with height of plate (5.29 cm);} \end{aligned}$$

$$\begin{aligned} \text{Draft} &= 10.47 \text{ cm} \\ \text{Freeboard} &= 4.82 \text{ cm} \end{aligned}$$